



HAL
open science

Anticancer boron-containing prodrugs responsive to oxidative stress from the tumor microenvironment

Hichem Maslah, Charles Skarbek, Stéphanie Pethe, Raphaël Labruère

► To cite this version:

Hichem Maslah, Charles Skarbek, Stéphanie Pethe, Raphaël Labruère. Anticancer boron-containing prodrugs responsive to oxidative stress from the tumor microenvironment. *European Journal of Medicinal Chemistry*, 2020, 207, pp.112670 -. 10.1016/j.ejmech.2020.112670 . hal-03492397

HAL Id: hal-03492397

<https://hal.science/hal-03492397>

Submitted on 26 Aug 2022

HAL is a multi-disciplinary open access archive for the deposit and dissemination of scientific research documents, whether they are published or not. The documents may come from teaching and research institutions in France or abroad, or from public or private research centers.

L'archive ouverte pluridisciplinaire **HAL**, est destinée au dépôt et à la diffusion de documents scientifiques de niveau recherche, publiés ou non, émanant des établissements d'enseignement et de recherche français ou étrangers, des laboratoires publics ou privés.



Distributed under a Creative Commons Attribution - NonCommercial 4.0 International License

Anticancer boron-containing prodrugs responsive to oxidative stress from the tumor microenvironment

Hichem Maslah, Charles Skarbek, Stéphanie Pethe, Raphaël Labruère*

Université Paris-Saclay, CNRS, Institut de chimie moléculaire et des matériaux d'Orsay, 91405, Orsay, France.

Keywords: Prodrug, anticancer chemotherapy, reactive oxygen species, boronic acids and esters.

* Corresponding author

E-mail address: raphael.labruere@universite-paris-saclay.fr (R. Labruère).

ABSTRACT

Boronic acid (and ester) prodrugs targeting the overexpressed level of reactive oxygen species within tumor microenvironment represent a promising area for the discovery of new selective anticancer chemotherapy. This strategy that emerged only ten years ago is exponentially growing and could demonstrate its clinical usefulness in the near future. Herein, the previously described small-molecule and macromolecular anticancer prodrugs activated by carbon-boron oxidation are gathered. This review reports on the most interesting derivatives mentioned in the literature based on the *in vitro* and *in vivo* activity when available. Eventually, the pharmacological applicability of this strategy is discussed, in particular, the kinetic aspect of the prodrug oxidation and the selectivity of this reaction towards certain ROS from the tumor microenvironment are specified.

1. Introduction

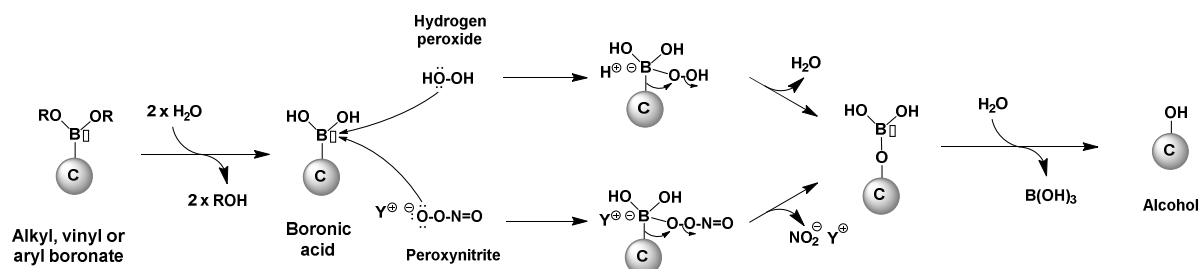
The prodrug strategy was initially introduced by Albert in 1958.[1] Prodrugs are activity-masked molecules designed to be activated *in vivo* by an enzymatic or a chemical reaction. In most cases, these molecules are covalent assemblies made of the active drug linked to a temporary moiety. The latter chemical unit confers new physicochemical properties to the entire entity optimizing its absorption, distribution, metabolism, excretion and toxicity (ADMET).[2–4] The prodrug strategy used in anticancer chemotherapy intends to deliver the active drug only at the tumor site in order to avoid deleterious side effects on normal tissues. Indeed, chemotherapies used in medical oncology are mostly cytotoxic agents and these drugs indifferently target both healthy and cancer cells. In this case, the temporary moiety must: (i) strongly impede the activity of a given antitumor agent; (ii) be specifically cleaved in cancer tissues to permit cancer-targeted drug delivery.[5–7]

Cancer cells are markedly different to cells from healthy tissues. The biologic singularities of cancer cells is therefore exploited in anticancer prodrug strategy in order to localize the delivery of the active drug at the tumor site. Abnormalities of the tumor environment has led to distinct strategies in cancer-responsive prodrug research. First, certain enzymes such as cathepsins are overexpressed in cancer cells and specific prodrugs were developed to target this

43 characteristic.[8–10] Prodrugs capitalizing on the hypoxia of cancer cells inside solid tumors
 44 are also the object of intensive research.[11–13] Antitumor targeted-prodrugs responsive to
 45 the pronounced oxidative stress in cancer cells have been recently developed.[14,15] Indeed,
 46 biological studies of tumors have revealed that cancer cells have a higher degree of oxidative
 47 stress compared to healthy cells.[16] This stress is produced by deregulated and enhanced
 48 mitochondrial functions and cellular metabolism. Oxidative stress stimulates the tumor
 49 progression processes such as cell proliferation and angiogenesis. Cancer cells migration and
 50 neovascularization will ultimately lead to the dissemination and growth of cancer cells in
 51 metastatic sites. Macrophages have been described to promote the generation of oxidative
 52 stress of cancer cells through the secretion of molecular mediators.[17] These immune cells
 53 are primarily present around the tumor cells in order to eradicate them by phagocytosis and
 54 production of oxygen-containing reactive molecules. Nonetheless, they will indirectly contribute
 55 to cancer progression.[18] These cellular events provide an increase of the oxygenated
 56 reactive molecules level in the tumor microenvironment.

57 These highly reactive molecules are composed of reactive oxygen species (ROS) and reactive
 58 nitrogen oxide species (RNOS).[16] Among ROS, superoxide anion ($O_2^{\cdot-}$) is engendered from
 59 O_2 via NADPH oxidase action and mitochondrial metabolism. $O_2^{\cdot-}$ is subsequently converted
 60 to hydrogen peroxide (H_2O_2) by superoxide dismutase (SOD) catalysis. H_2O_2 further evolves
 61 into hypochlorous acid (HOCl) and hydroxyl radical ($HO\cdot$). Among RNOS, nitric oxide ($NO\cdot$) is
 62 produced by reaction of molecular oxygen and L-arginine catalyzed by nitric oxide synthases
 63 (NOSs). $NO\cdot$ spontaneously reacts with $O_2^{\cdot-}$ to form peroxynitrite/peroxinitrous acid ($ONOO^-$
 64 / $ONOOH$). The latter species is unstable and generate hydroxyl radical and nitrogen dioxide
 65 radical ($NO_2\cdot$).

66 Boronic acids and their corresponding esters have been developed as temporary masking
 67 groups for drugs or probes specifically triggered by oxygen-containing reactive molecules.[19–
 68 23] In biological aqueous media, boronate esters are rapidly hydrolyzed into boronic acid.[24]
 69 Among the different reactive species, hydrogen peroxide, hypochlorite anion ($ClO\cdot$) and
 70 peroxynitrite were shown to react with boronic acids and esters to further oxidize the carbon-
 71 boron bond to form an alcohol group.[25] In biological conditions, hypochlorite anion will almost
 72 exclusively react with cellular amines and thiols since the latter reactions will be faster than the
 73 oxidation of carbon-boron bonds. Nucleophilic oxygen of the reactive species will be able to
 74 attack the empty p orbital of the boron atom (Scheme 1).[26,27] Carbon migration to oxygen
 75 further gives a borate that will be hydrolyzed to afford the corresponding alcohol and non-toxic
 76 boric acid.[28] At physiological pH, conversion by peroxynitrite is 10^6 times faster than the
 77 hydrogen peroxide-mediated oxidation likely due to the anionic form of peroxynitrite in
 78 comparison to neutral H_2O_2 . [25]

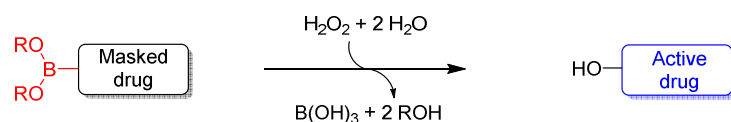


79
 80 **Scheme 1.** Mechanism of boronic acid oxidation into alcohol by either hydrogen peroxide or
 81 peroxynitrite.

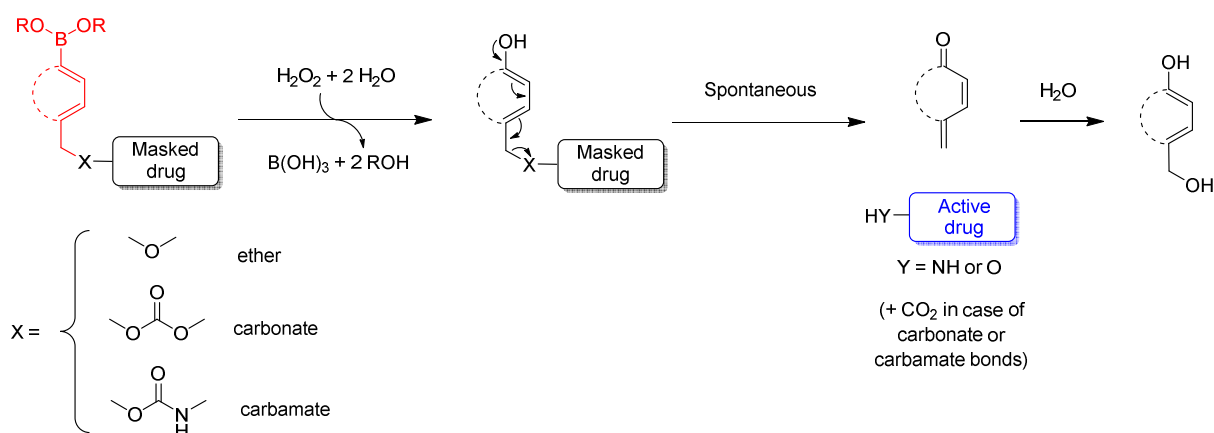
82
 83

84 The boronic/boronates functionalities were used as temporary moieties to either mask aliphatic
 85 alcohols,[25,29] enols[30,31] or aryl-alcohols.[19,23] The active effector can be connected to
 86 the boronic/boronates groups directly or via self-immolative spacers.[32,33] The use of these
 87 spacers allows the bounding of different effectors through either their alcohol or amine
 88 functions generating ether, carbonate or carbamate bonds. The volume added by the spacer
 89 to the final entity contributes to a better masking of the biological activity. Oxidation of such
 90 spacer lead to the formation of an aryl-alcohol motif that will undergo spontaneous elimination
 91 leading to the release of an effector (Scheme 2).

Boronic/boronate prodrug



Arylboronic/boronate prodrug



96 **Scheme 2.** Release of the active drug from boron-containing prodrug by either direct C-B
 97 bond oxidation or by oxidation and subsequent self-immolative process.

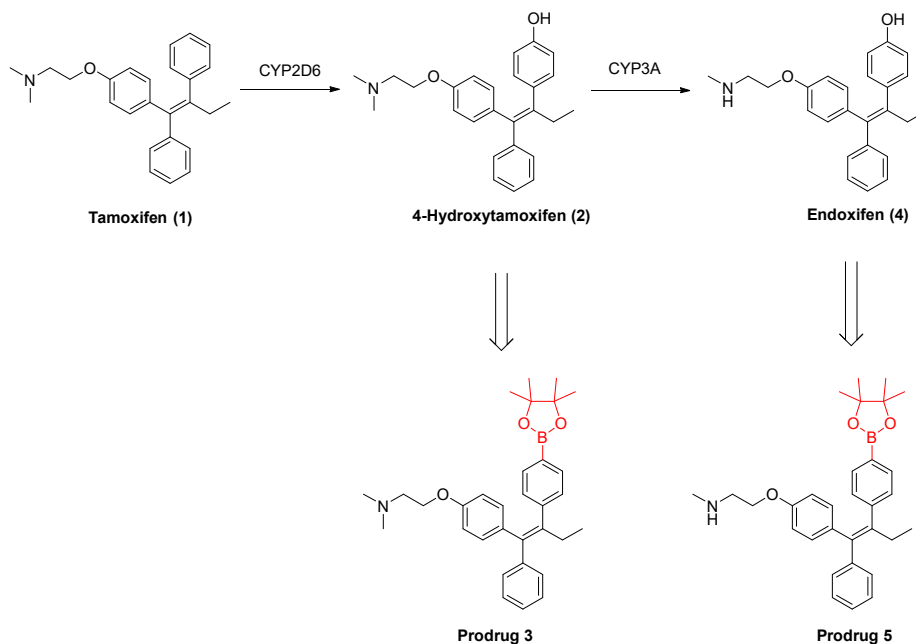
98
99 The strategy of boronic acid/boronate oxidation has been widely used for the emergence of
 100 many probes for tumor imaging and/or prodrugs with tumor targeting properties leading to the
 101 release of the parent drug. Herein, we comprehensively review the ROS responsive boronate
 102 prodrugs that were developed and evaluated as anticancer agents. In the next section, we
 103 gathered the different platforms used to construct the prodrug of interest: a majority of small
 104 molecules were found but a non-negligible amount of drug delivery-based polymeric matrix
 105 and nanoparticles were also described.

106 107 2. Small-molecule and macromolecular prodrugs

108 109 Precursors of selective estrogen receptor modulators (SERM)

110 The selective estrogen receptor modulators have been developed to treat breast cancer
 111 tumors presenting the estrogen receptor.[34] Antiestrogens, such as tamoxifen **1**, bind to the
 112 hormone receptor and block the proliferation of the cancer cells. Moreover, tamoxifen **1** is a
 113 prodrug converted to both 4-hydroxytamoxifen **2** and endoxifen **4** by cytochrome P450

114 enzymes. The Wang group has therefore synthesized and evaluated boron-based prodrugs of
115 4-hydroxytamoxifen **2** and endoxifen **4** as potential anticancer agents (Scheme 3).[35–37]



116

117 **Scheme 3.** Structures of 4-hydroxytamoxifen and endoxifen (oxidative metabolites of
118 tamoxifen) and their prodrugs.

119

120 This strategy is indeed meaningful since these two active metabolites would be similarly
121 obtained by oxidative cleavage of the boronic acid function of **3** and **5** in the tumor environment.
122 In vitro cytotoxic activity of **3** and **5** was determined against MCF-7 and T47D, two breast
123 cancer cell lines expressing the estrogen receptor. The prodrug **3** and its active metabolite 4-
124 hydroxytamoxifen **2** were as active against a given cell line. 80% conversion of prodrug **3** to 4-
125 hydroxytamoxifen **2** was observed in cell culture media and the cellular uptake of **3** was 4 times
126 higher than 4-hydroxytamoxifen **2** in MCF-7 culture. Comparable in vitro observations were
127 made for the prodrug/drug couple: **5**/endoxifen **4**. Growth inhibition of MCF-7 cancer
128 xenografts in mice was similar for the prodrug **5** and the active metabolite endoxifen **4** at the
129 optimal dose of 1 mg/kg. Metabolism and pharmacokinetic studies in mice showed that the
130 plasma concentration of boronic prodrugs **3** and **5** were 40-fold higher than their respective
131 active ingredients or the other parent prodrug tamoxifen **1** administered at the same dose.
132 Noteworthy, the conversion of both prodrugs was due to the oxidation of the boronic acid
133 functions by cytochrome P450 enzyme rather than the ROS/RNOS overexpressed by cancer
134 cells. The enhanced bioavailability from the prodrugs **3** and **5** is therefore due to the prolonged
135 release of the phenol counterparts. Hence, rapid excretion of 4-hydroxytamoxifen **2** and
136 endoxifen **4** is observed when these molecules are directly injected and this was attributed to
137 the glucuronidation of the hydroxy groups during phase II metabolism.

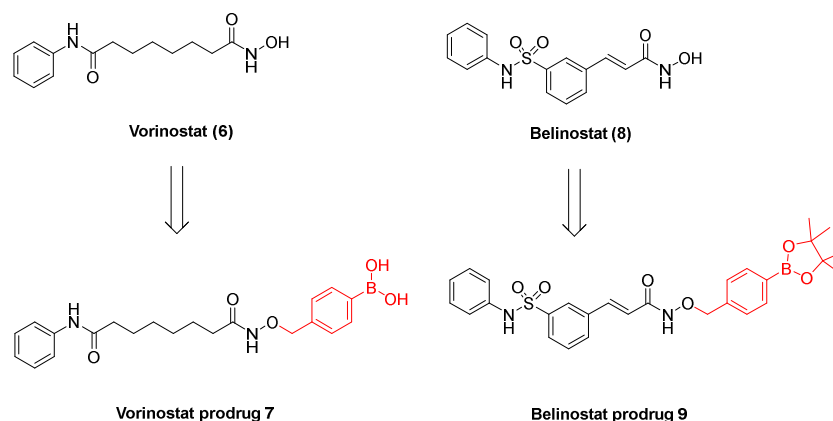
138

139 Precursor of epigenetic regulators

140 Histone deacetylase (HDAC) inhibitors

141 Histone deacetylases (HDACs) remove acetyl groups from histone and other nonhistone
142 targets. HDACs control the transcription of oncogenes leading to the production of proteins
143 involved in cancer induction and proliferation and HDAC inhibitors were developed to prevent

144 the progression of cancer cells.[38] Interestingly, two hydroxamate molecules: vorinostat **6** and
145 belinostat **8**, FDA-approved drugs for the treatment of cutaneous T-cell lymphoma, were the
146 basis for the preparation of prodrugs (Scheme 4).[39,40] Indeed, these pharmaceuticals are
147 good candidates for prodrug development since they present important drawbacks such as
148 toxicity and weak bioavailability due to both the lack of hydroxamic acid stability and to rapid
149 excretion by sulfation and glucuronidation. Liao et al.[39] proposed the prodrug **7** of vorinostat
150 **6** targeting the acute myeloid leukemia owing to the high level of ROS produced by these tumor
151 cells.[41]



152

153

Scheme 4. Prodrugs of vorinostat and belinostat.

154

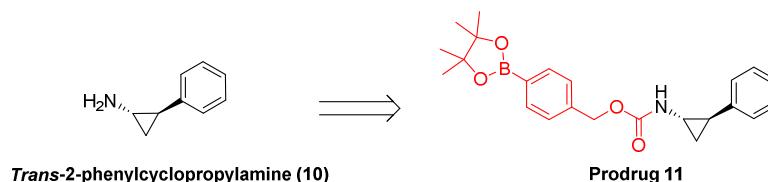
155 Here, the drug was linked to a self-immolative benzene boronic acid moiety to afford the
156 prodrug **7**. The viability of two leukemia cell lines, U937 and MV4-11, treated by **7** and
157 vorinostat **6** was determined in vitro and showed a partial recovery (~ 20%) of the drug activity
158 after incubation.

159 Furthermore, Wang and colleagues prepared a prodrug **9** made of a benzene boronate nucleus
160 branched to the hydroxamic acid moiety of belinostat **8** for the chemotherapy of solid
161 tumors.[40] Belinostat **8** and **9** were tested in vitro against four cancer cell lines: A549 (lung
162 carcinoma), HeLa (cervical cancer) and, MDA-MB-231 and MCF-7 (breast adenocarcinoma).
163 Again, around 25% of the parent drug activity was recovered after incubation except for the
164 MCF-7 cells where prodrug **9** displayed only 5% of the corresponding drug activity. Conversion
165 of the prodrug **9** into belinostat **8** in MDA-MB-231 culture cell media was ~ 10% after 24h of
166 incubation. The HDAC inhibitory activity of the prodrug **9** was then measured and was ten
167 times lower than that of belinostat **8**. Altogether, these observations account for the noticeable
168 difference of cancer cells viability between the drug and the prodrug. In vivo activity of prodrug
169 **9** was compared to belinostat **8** in a MCF-7 xenograft model in mice at the dose of 10
170 mg/kg/day, a slight increase of efficacy was observed for **9** toward the free drug. The belinostat
171 **8** concentration was twice higher in tumor tissue after prodrug **9** subcutaneous injection in
172 contrast with the same injected dose of the parent drug. The higher efficacy of the prodrug is
173 explained by the increased bioavailability of the benzene boronate precursor **9**. The plasmatic
174 concentration in mice was quantified for both belinostat **8** and its prodrug **9**: 10 mg/kg were
175 independently injected and after 3h, the concentration of belinostat **8** was 7-fold higher when
176 using the prodrug **9**. [42] Moreover, study of **9** metabolism in liver S9 fraction clearly brought to
177 light the role of the enzymatic metabolism (via cytochrome P450) in the conversion of the
178 boronic acid function into the corresponding phenol leading to belinostat **8** through self-
179 immolation.

180

181 Lysine-specific histone demethylase inhibitor

182 Among histone post-translational modifications, lysine methylation of histone governs the
183 structure of chromatin and the methylation degree of histones is involved in cancer
184 formation.[43] Lysine-specific histone demethylase inhibitor are not currently used in clinic but
185 these molecules are studied for the development of anticancer epigenetic drugs. Engel et
186 al.[44] have prepared a benzene boronate prodrug **11** of the promising histone demethylase
187 inhibitor *trans*-2-phenylcyclopropylamine **10** (Scheme 5).



189 **Scheme 5.** Prodrug of *trans*-2-phenylcyclopropylamine.

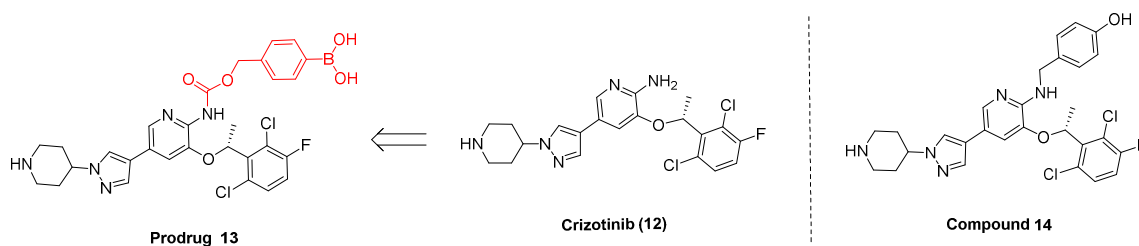
190

191 Prodrug **11** was tested in vitro against glioblastoma U87 cells and primary glioblastoma cells,
192 and healthy astrocytes. No activity was observed up to 300 μ M on healthy astrocytes while
193 primary glioblastoma and U87 cells were impacted at 10 μ M and 1 μ M respectively. The
194 authors also showed the impact of the quinone methide (formed from the benzene boronate
195 promoiety) which reacts covalently with glutathione in cells reducing the intracellular
196 concentration of this antioxidant (vide infra).

197

198 **Precursor of tyrosine kinase inhibitors**

199 Crizotinib **12** is a tyrosine kinase inhibitor developed to treat non-small cell lung cancers.[45]
200 This drug however presents important side effects such as hepatotoxicity and neutropenia.
201 These drawbacks prompted the Kowol group to prepare a benzene boronate prodrug **13** of
202 this molecule in an attempt to selectively reach the cancer cells (Scheme 6).[45]



204

204 **Scheme 6.** Benzyloxycarbonyl prodrug of crizotinib and non-immolated metabolite **14**.

205

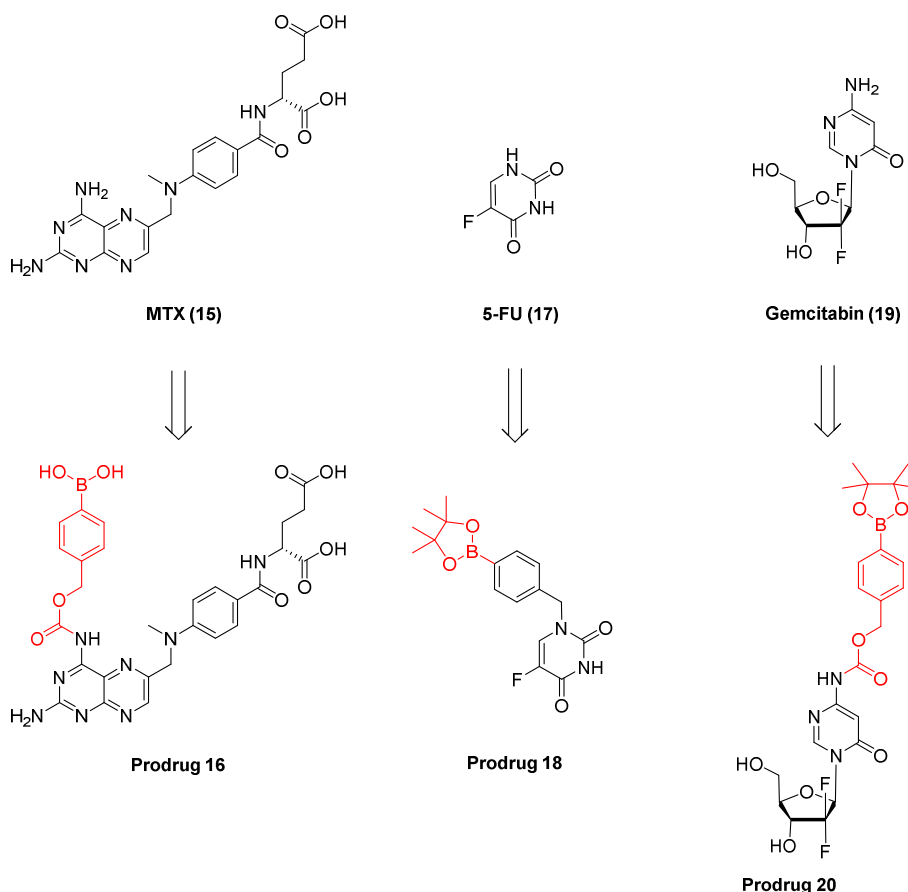
206 Three non-small cell lung cancer cell lines (H1993, RUMH and H2228) known to respond to
207 crizotinib **12** were evaluated toward their production of ROS by flow cytometry using 2',7'-
208 dichlorofluorescein diacetate. The in vitro ROS production of the H1993 cells was found to be
209 twice as much as the two other cell lines. In vitro cytotoxicity assays showed that approximately
210 50% of free crizotinib **12** ($IC_{50} \sim 3-15 \mu$ M) activity was found with the prodrug **13**. Addition of
211 H_2O_2 prior to incubation with the different cell lines completely restored the activity of the
212 original drug, except when in contact with H1993 cells where the activity remains surprisingly
213 lower. The authors also observed that a stable non-immolated metabolite **14**, a *p*-

214 hydroxybenzyl adduct of crizotinib was as active as the free drug against all the tested cell
215 lines pointing out that benzyl moiety is not sufficient to mask the drug activity in this case.

216

217 Precursors of antimetabolite drugs

218 Methotrexate (MTX) **15**, a potent inhibitor of the dihydrofolate reductase implied in the purine
219 and pyrimidine synthesis, is used in clinic to treat cancer and autoimmune diseases. The
220 Clausen group has described several benzene boronate prodrugs of methotrexate **15** originally
221 developed for the treatment of rheumatoid arthritis (Scheme 7).[46,47]



222

223

224

225 Recently, the in vitro activity of the prodrug **16** (Scheme 7) was reported on HL-60 (human
226 leukemia cancer cell line), HeLa cancer cell line and HEK293 (human embryonic kidney cell
227 line).⁴⁷ The HL-60 cells were shown to produce around ten times more ROS in vitro than of the
228 HEK293 cells. However, prodrug **16** displayed close in vitro activity against the two latter cell
229 lines (IC₅₀ ~ 0.05 μM), a growth inhibition decreased by a factor 2-4 in comparison with the
230 free methotrexate **15**.

231 The antimetabolite 5-fluorouracil (5-FU) **17**, a widely used antitumor drug, presents several
232 side effects such as myelosuppression and neurotoxicity. In order to reduce these drawbacks,
233 the Xue group has developed the benzene boronate prodrug of 5-fluorouracil (Scheme 7).[48]
234 Boronate prodrug **18** and its corresponding boronic acid were tested in vitro against the 60
235 cancer cell lines from the National Cancer Institute. Prodrug **18** was more active against all cell
236 lines than its boronic acid counterpart which is quite surprising since boronate esters are

237 hydrolyzed into boronic acid in aqueous media (vide supra). Then, the authors particularly
238 compared breast cancer cells MCF-7 to immortalized mouse embryonic epicardial cells MEC1.
239 5-Fluorouracil **17** was cytotoxic against two cell lines with an IC₅₀ around 1 μM whereas **18**
240 had no effect against MEC1 up to a concentration of 100 μM and was slightly active on the
241 MCF-7 cancer cells (IC₅₀ = 10-50 μM). Aside from that, prodrug **18** showed a better drug safety
242 profile than 5-fluorouracil **17** on wild-type C57BL/6 male mice.

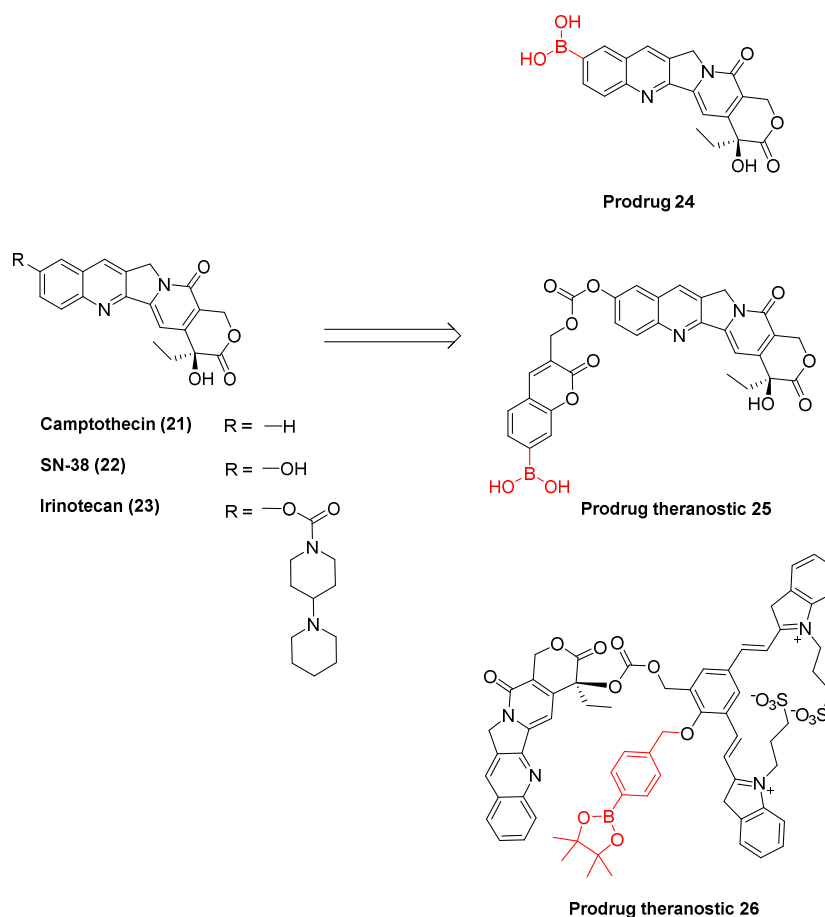
243 Another nucleotide analog used in clinic, gemcitabin **19**, was linked to a benzene boronate
244 moiety to build the prodrug **20** (Scheme 7).[49] Gemcitabin **19** and prodrug **20** were evaluated
245 in vitro against pancreatic cell lines: cancerous (PSN1 and BxPC3) and normal (NPEC). The
246 H₂O₂ level produced by each cell line was measured using the ROS-Glo™ assay which
247 demonstrated a weakly higher production of ROS by the cancer cells. Gemcitabin **19** displayed
248 an IC₅₀ of 0.005-0.015 μM against the three cell lines and prodrug **20** was around 20 times
249 less active in each case. Nonetheless, prodrug **20** was able to retrieve the activity of gemcitabin
250 **19** when ROS were artificially produced by the cancer cell lines via preliminary addition of 2-
251 deoxy-D-glucose. In vivo activity was determined using PSN1 xenograft model in mice and
252 showed a similar activity of both gemcitabin **19** and prodrug **20**. However, myelosuppression
253 was lowered in mice treated with the prodrug **20** and the authors showed that concentration of
254 the resulting gemcitabin **19** in bone marrow was reduced in comparison with the gemcitabin-
255 treated group.

256

257 **Precursors of cytotoxic drugs**

258 **Camptothecin 21**

259 Camptothecin **21** is a strongly cytotoxic natural product as a result of its topoisomerase I
260 inhibitory activity. The 10-hydroxycamptothecin known as SN-38 **22**, is the toxic hydrolytic
261 metabolite of the commercialized prodrug irinotecan **23**. [50] Thus, Lei et al. [51] prepared the
262 oxidative prodrug **24** of SN-38 **22** by replacing the original phenol group into a boronic acid
263 function (Scheme 8).



264

265

Scheme 8. Prodrugs of camptothecin.

266

267 Prodrug **24** and the corresponding active metabolite SN-38 **22** were tested in vitro against six
 268 cancer cell lines: colon cancer cells HCT-15 and HT-29, breast cancer cells MCF-7 and MDA-
 269 MB-231 and, glioblastoma cells U87MG and U251. The activity of SN-38 **22** was fully restored
 270 upon incubation of **24** with the different cell lines (IC_{50} ranging from 0.01 to 5 μ M). The authors
 271 observed that the conversion of **24** into SN-38 **22** in MCF-7 culture cell media was around 40%
 272 after 48h of incubation. Moreover, the topoisomerase I inhibitory evaluation of **24** showed that
 273 the boronic acid derivative was as potent as SN-38 **22**. These two latter observations therefore
 274 account for the good in vitro activity of **24** against this panel of cancer cells. Prodrug **24** was
 275 evaluated in vivo using U87MG cancer xenograft in mice and displayed a modest efficacy at 2
 276 mg/kg in comparison with the reference irinotecan **23** (antitumor effect of 8% T/C with
 277 irinotecan vs. 28% T/C with **24**).

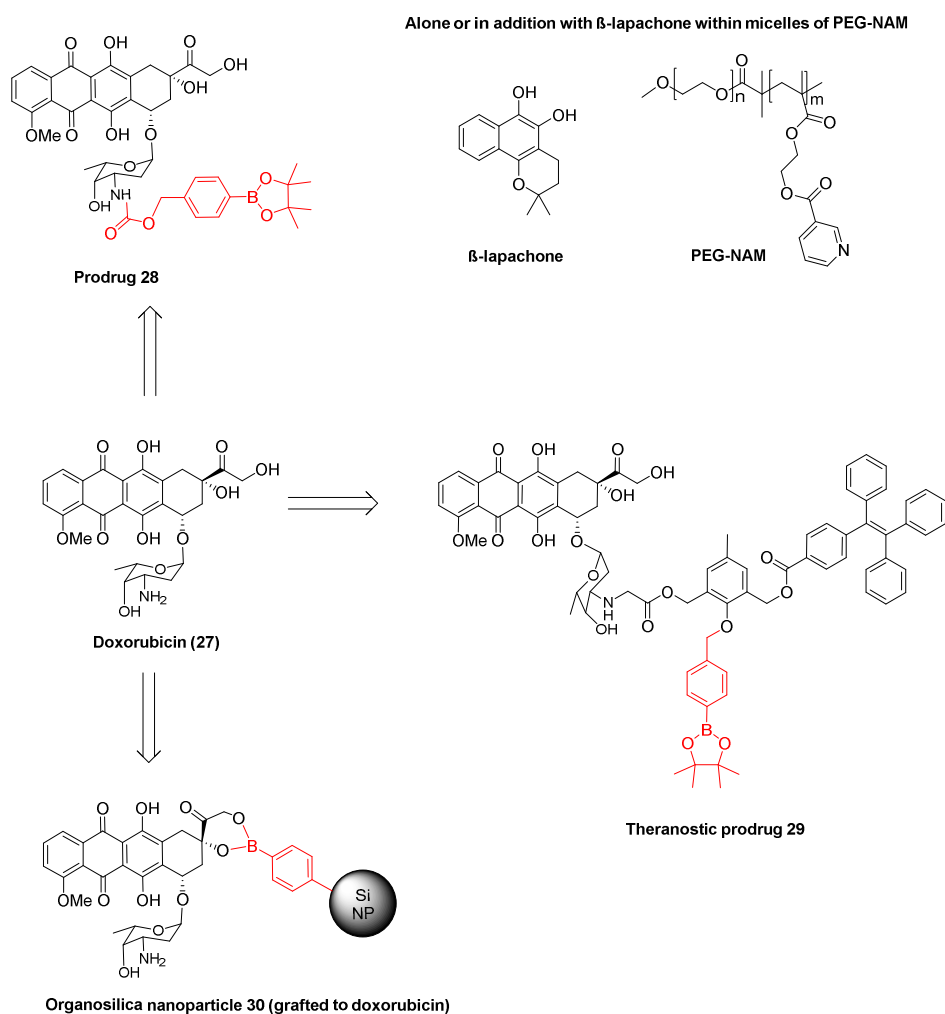
278 Theranostic boronate-based prodrugs of camptothecin were also prepared. In cancer
 279 chemotherapy, this approach combining therapy and diagnosis allows the visualization of the
 280 drug by imaging its localization within the organism. The Kim group prepared a prodrug **25**[52]
 281 able to release a fluorophore (a coumarin) and SN-38 **22** whereas the Shabat group developed
 282 a precursor **26** liberating a near-infrared cyanine fluorophore and camptothecin **21** (Scheme
 283 8).[53] Prodrug **25** and SN-38 **22** were evaluated in vitro against melanoma cells B16F10 and
 284 cervical cancer cells Hela. The prodrug **25** was able to restore around 60% of the SN-38 **22**
 285 activity on both cancer cells and a complete recovery was obtained when adding 100 μ M of
 286 H_2O_2 . This latter observation was made at 100 μ M of tested compounds, a concentration way
 287 beyond the IC_{50} of SN-38 **22**. The authors treated a B16F10 melanoma xenograft in mice with

288 **25** at 0.25 mg/kg or with a saline solution. Again, a relatively limited efficacy was observed with
 289 a slightly prolonged survival time (1-6 days) of the treated mice over the non-treated group.
 290 Regrettably, irinotecan **23** or the active ingredient SN-38 **22** were not evaluated in this in vivo
 291 study. In regards to the cyanine prodrug **26**, the activity against U87MG cells was first
 292 determined in vitro: the authors observed an IC₅₀ of 0.25 μM for the prodrug **26** whereas
 293 camptothecin **21** was ten times more active (IC₅₀ = 0.02 μM). Nonetheless, the pre-incubation
 294 of H₂O₂ with **26** lead to the full release of camptothecin **21** and therefore the original IC₅₀ of
 295 this free drug was re-established. In vivo imaging of the prodrug **26** using U87MG cancer
 296 xenograft in mice showed a precisely localized activation within the tumor after intratumoral
 297 administration. The fluorescence appeared only one minute after prodrug injection and the
 298 cyanine dye was still observable 6 hours after administration to the mice.

299

300 Doxorubicin **27**

301 Doxorubicin **27** is a cytotoxic natural product acting as DNA intercalating agent and
 302 topoisomerase II inhibitor (Scheme 9). Although used in clinic as antitumor drug, important
 303 side effects such as cardiotoxicity were described.[54] Our group therefore prepared
 304 arylboronate-based prodrugs of doxorubicin by branching the free amine function of this
 305 drug.[55]



306

307

Scheme 9. Prodrugs of doxorubicin.

308

309 First, using an arylboronate profluorescent probe of coumarin, we determined the most efficient
310 cell line at converting the probe into free coumarin among a panel of six cancers from different
311 organs (breast cancer MCF-7 and the resistant counterpart MCF-7 MDR, hepatocellular
312 carcinoma Hep G2, lung adenocarcinoma A549, glioblastoma U87, pancreatic cancer cell line
313 MiaPaCa-2). Hep G2 and MiaPaCa-2 were the most ROS-producing cell lines but the
314 cytotoxicity of the prodrugs was nonetheless evaluated on the different cell lines. Prodrug **28**
315 was the most interesting since it displayed an IC_{50} of 0.3 μ M corresponding to 67% of the total
316 effect obtained with the same concentration of doxorubicin **27** (IC_{50} = 0.2 μ M). Using MiaPaCa-
317 2 pancreatic tumor in ovo xenograft via the HET-CAM (Hen's Egg Test-Chorioallantoic
318 Membrane) assay, **28** induced the same tumor regression as doxorubicin **27** intratumorally
319 injected at the same dose. Ye et al.[56] have efficiently entrapped the prodrug **28** in polymeric
320 nanoparticles of polyethylene glycol conjugated to niacin (PEG-NAM, Scheme 9). The ROS
321 generator β -lapachone was co-encapsulated within the micelles in order to enhance the
322 release of free doxorubicin. The authors observed that β -lapachone was first liberated and was
323 then able to amplify the conversion of **28** into doxorubicin **27**. The loaded nanoparticles
324 together with doxorubicin **27**, β -lapachone and **28** were evaluated in vitro against three breast
325 cancer cell lines (4T1, MCF-7 and MCF-7 ADR, i.e resistant to doxorubicin) and against
326 NIH/3T3 fibroblasts. Prodrug **28** was less active than doxorubicin **27** showing weak in vitro
327 conversion of **28** into free drug against the four cell lines. Furthermore, the IC_{50} s of
328 doxorubicin **27**, β -lapachone and the loaded nanoparticles obtained were equals in every
329 cases except with the resistant MCF-7 cells where the micelles and β -lapachone were 4-5
330 times more active. This last observation highlight the particular efficacy of the latter molecules
331 against doxorubicin resistant cancer cells. In vivo pharmacokinetics assays showed that both
332 bioavailability and tumor concentration of doxorubicin **27** is improved when the doxorubicin-
333 containing polymeric micelles are injected to mice in comparison with the administration of free
334 drug at the same dose. The different molecules were tested on a MCF-7 ADR tumor xenograft
335 model by intravenous injections at 5 mg/kg. An important tumor regression was observed (~
336 90%) when treated with doxorubicin **27** loaded nanoparticles which was higher than the free
337 doxorubicin **27** (~ 50%) and prodrug **28** (~ 30%).

338 A theranostic prodrug **29** of doxorubicin was built based on a central benzenic self-immolative
339 spacer able to release simultaneously the free drug and a fluorophore, a tetraphenylethene
340 with aggregation-induced emission properties (Scheme 9).[57] The construct **29** was evaluated
341 in vitro on Hela cells that were first treated with 1-phorbol-12-myristate-13-acetate (PMA), an
342 agent inducing the ROS production in cells. After incubation, fluorescence and cytotoxicity
343 (IC_{50} ~ 2 μ M) were observed in PMA-treated cells whereas no effect was detected on the PMA-
344 free cells.

345 Organo-silica nanoparticles **30** displaying phenyl boronic moiety at their surface were prepared
346 by the Shi group.[58] Doxorubicin was then covalently linked via its cis diol part to generate a
347 boronate ester bond leading to nanoparticles covered with the drug (Scheme 9). These
348 nanoparticles were designed to specifically release the doxorubicin within a tumor by ROS-
349 mediated oxidation or by acidic cleavage of the boronate ester bond (due to particularly acidic
350 pH in cancer cells). Hyaluronic acid was also coated at the surface of the nanoparticles in order
351 to specifically target the CD44 receptor which is overexpressed at the surface of certain cancer
352 cells. Efficient in vitro release of doxorubicin **27** was first demonstrated in presence of H_2O_2
353 and then the particles were evaluated against Hep G2 cancer cells (CD44 $^{+++}$) and NIH/3T3
354 fibroblasts (CD44 $^{+}$). Nanoparticles **30** bearing hyaluronic acid and doxorubicin were: (i) more
355 toxic against Hep G2 (IC_{50} ~ 0.5 μ M) than their hyaluronic acid free counterparts (IC_{50} = 2 μ M)
356 and (ii) more active against Hep G2 than NIH/3T3 (IC_{50} ~ 2 μ M).

357

387

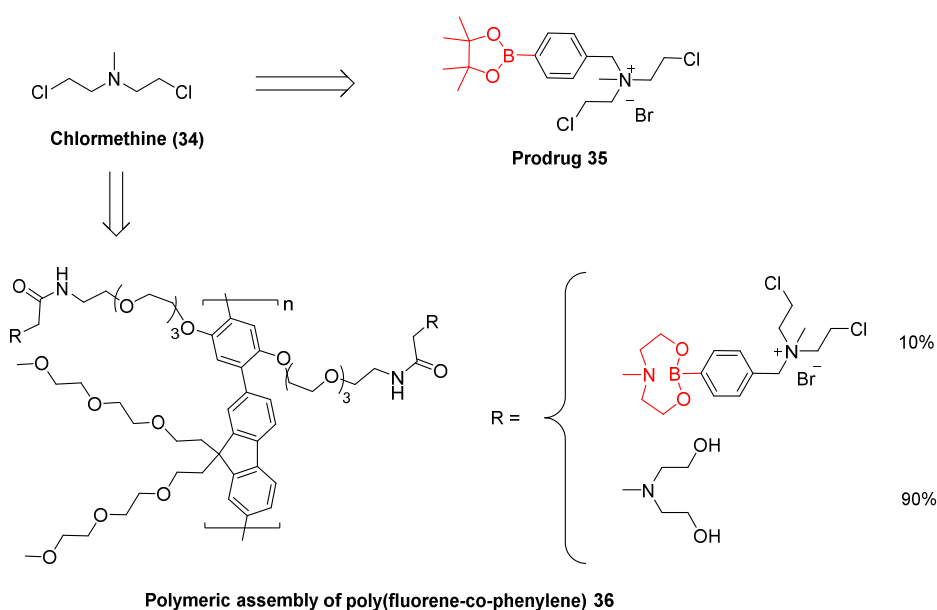
388 Theranostic prodrug **33** was evaluated in vitro against MRC5 fibroblasts and three cancer cell
389 lines: A549, HeLa, MDA-MB-231. Incubation with the cancer cells, in particular with A549,
390 showed greater conversion of **33** into turned-on coumarin and nitric oxide using fluorescence
391 microscopy experiment. A similar activity was observed against all three cell lines ($IC_{50} \sim 10$
392 μM) and a lower effect was noted on the MRC5 cells ($IC_{50} \sim 25 \mu M$).

393

394 Precursors of DNA alkylating agents

395 Nitrogen mustards

396 Nitrogen mustards are cytotoxic drugs reacting with DNA to form interstrand cross-links (ICLs).
397 The Peng group designed and synthesized benzene boronate prodrugs of chlormethine **34**
398 since this drug is weakly selective of cancer cells (Scheme 12).[62]



399

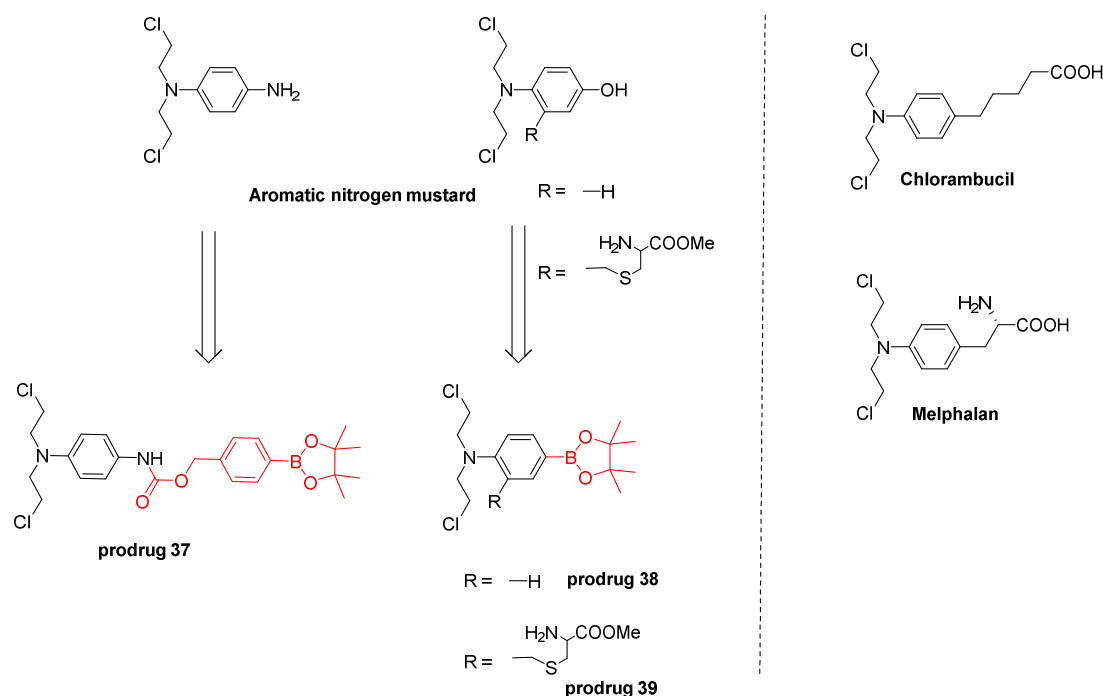
400

Scheme 12. Prodrugs of chlormethine.

401

402 When linked to benzene boronate, chlormethine is not able to form the electrophilic aziridinium
403 cycle strongly reacting with DNA. In vitro, prodrug **35** showed efficient ability to alkylate DNA
404 in presence of H_2O_2 and **35** was further evaluated against four cancer cells: leukemia cells SR,
405 lung cancer cells NCI-H460, renal cancer cells SN12C and CAKI-1, and healthy lymphocytes.
406 Prodrug **35** (with no added H_2O_2) was especially active against SR and NCI-H460 cells with
407 85-90% of growth inhibition at $10 \mu M$ while no activity was detected at this concentration on
408 the normal lymphocytes. Rationally, the same activity for **35** and its corresponding free boronic
409 acid was found in vitro against all cell lines. This benzene boronate prodrug of chlormethine
410 **34** was further bonded to a polymeric assembly of poly(flourene-co-phenylene) by Li et al.[63]
411 The polymeric prodrug **36** (Scheme 12) can be considered as theranostic since the polymer
412 backbone is fluorescent and was visualized into cells by imaging. The polymeric prodrug **36**
413 was tested on HeLa and A549 cells, and globally, **36** displayed a similar level of cytotoxicity as
414 prodrug **35** (i.e 80% of growth inhibition at $10 \mu M$).

415 Using a closely related strategy as earlier, Peng and co-workers prepared boronate prodrugs
 416 of aromatic nitrogen mustards where the electron-withdrawing boronate function was either
 417 directly linked to the effector (**38** and **39**) or via a benzyl self-immolative spacer (**37**) (Scheme
 418 13).[64,65]

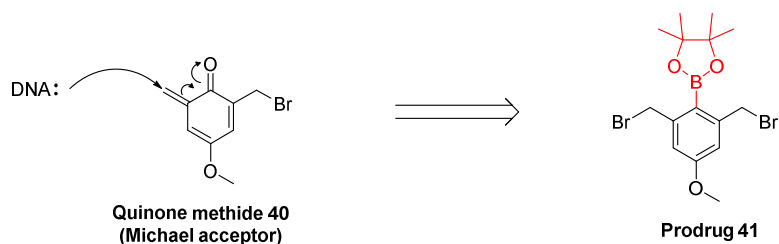


419
 420 **Scheme 13.** Structures of chlorambucil, melphalan and the prodrugs of aromatic nitrogen
 421 mustard.

422
 423 Amongst the synthesized prodrugs, prodrug **37** and **38** were the most active at forming ICLs
 424 and at inhibiting the panel of 60 cancer cells from the NCI. In particular, IC_{50} s of both prodrugs
 425 **37** and **38** were obtained below 1 μM against SR and NCI-H460 cells. Analogs of prodrugs **38**
 426 bearing a substituent were synthesized to further optimize the antitumor activity of this
 427 series.[66] Prodrug **39** displaying a cysteinyl methyl ester motif was shown to enhance the
 428 water solubility and cell permeability. Moreover, **39** was more effective in vitro against MDA-
 429 MB-468 than **38** and the reference drugs chlorambucil and melphalan. Prodrug **39** was
 430 evaluated in vivo using MDA-MB-468 cancer xenograft in mice and displayed significantly
 431 reduced tumor growth compared to the vehicle with no side effects.

432
 433 Quinone methides as alkylating agents

434 The Peng group also envisioned the generation of quinone methides as Michael acceptor for
 435 DNA strand (Scheme 14).[67–69] Among several benzene boronate precursors, prodrug **41**
 436 was the most interesting of their series.



437

438

Scheme 14. Prodrug of quinone methide as Michael acceptor.

439

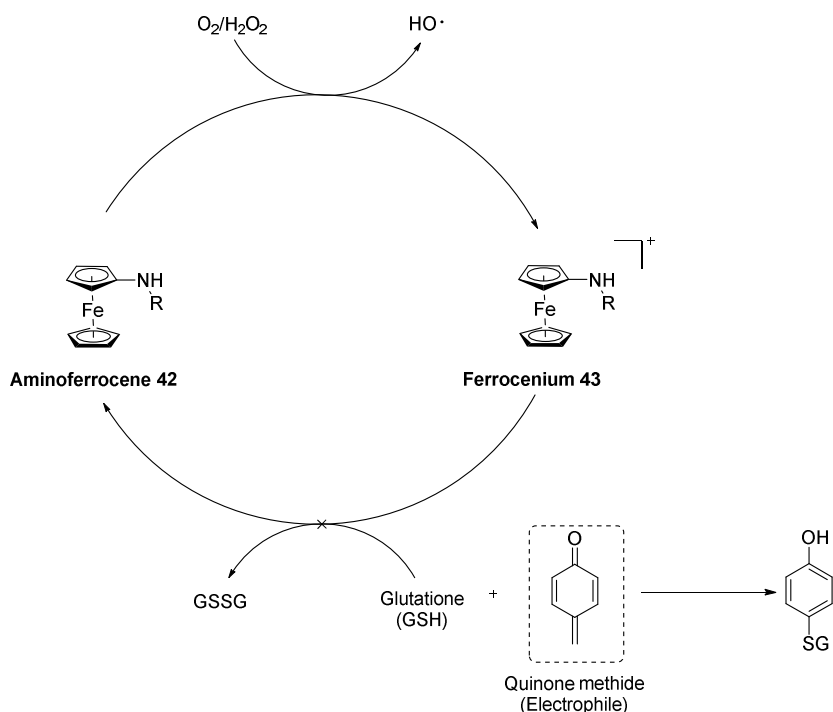
440 Prodrug **41** was able to form ICLs in presence of H_2O_2 and its cytotoxicity was evaluated
 441 against the NCI cancer cells panel. IC_{50} s of **41** against several cancer cells was about 10-20
 442 μM which was significantly more active than chlorambucil and melphalan.

443

444 **Precursors of ROS/RNOS amplifier/accumulator for oxidation therapy**

445 Aminoferrocene

446 Over the last decade, the group of Mokhir has developed benzene boronate precursors of
 447 aminoferrocene.[70–79] These precursor were conceived to increase drastically ROS
 448 concentrations inside cancer cells leading ultimately to cell death, i.e oxidation therapy.[80]
 449 The released aminoferrocene **42** reacts with hydrogen peroxide or oxygen to afford both
 450 cytotoxic hydroxyl radical and ferrocenium ion **43** (Scheme 15). These ROS are usually
 451 detoxified by antioxidants such as glutathione but in this strategy, electrophilic quinone methide
 452 is also formed and acts as glutathione scavenger blocking this protective mechanism.

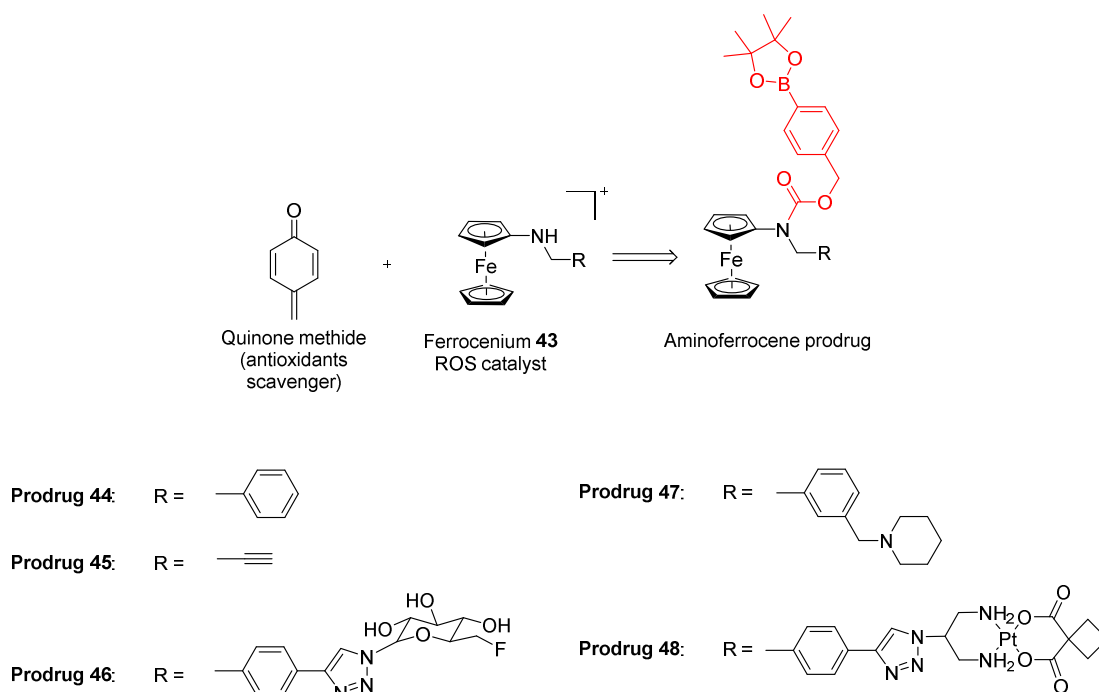


453

454 **Scheme 15.** Cycle for ROS amplification within tumor environment initiated by the presence
 455 of free aminoferrocene.

456

457 From a first series of aminoferrocene prodrugs,[70] the authors found that the prodrug **44**
 458 (Scheme 16) was the most efficient at both penetrating and amplifying ROS within HL-60
 459 leukemia cells. This is attributable to the greater stability of the liberated *N*-
 460 benzylaminoferrocene and **44** was indeed the most cytotoxic prodrug against HL-60 ($IC_{50} = 9$
 461 μM) whereas no activity was found against healthy fibroblasts ($IC_{50} > 100 \mu M$).



462
 463 **Scheme 16.** Aminoferrocene prodrugs.
 464

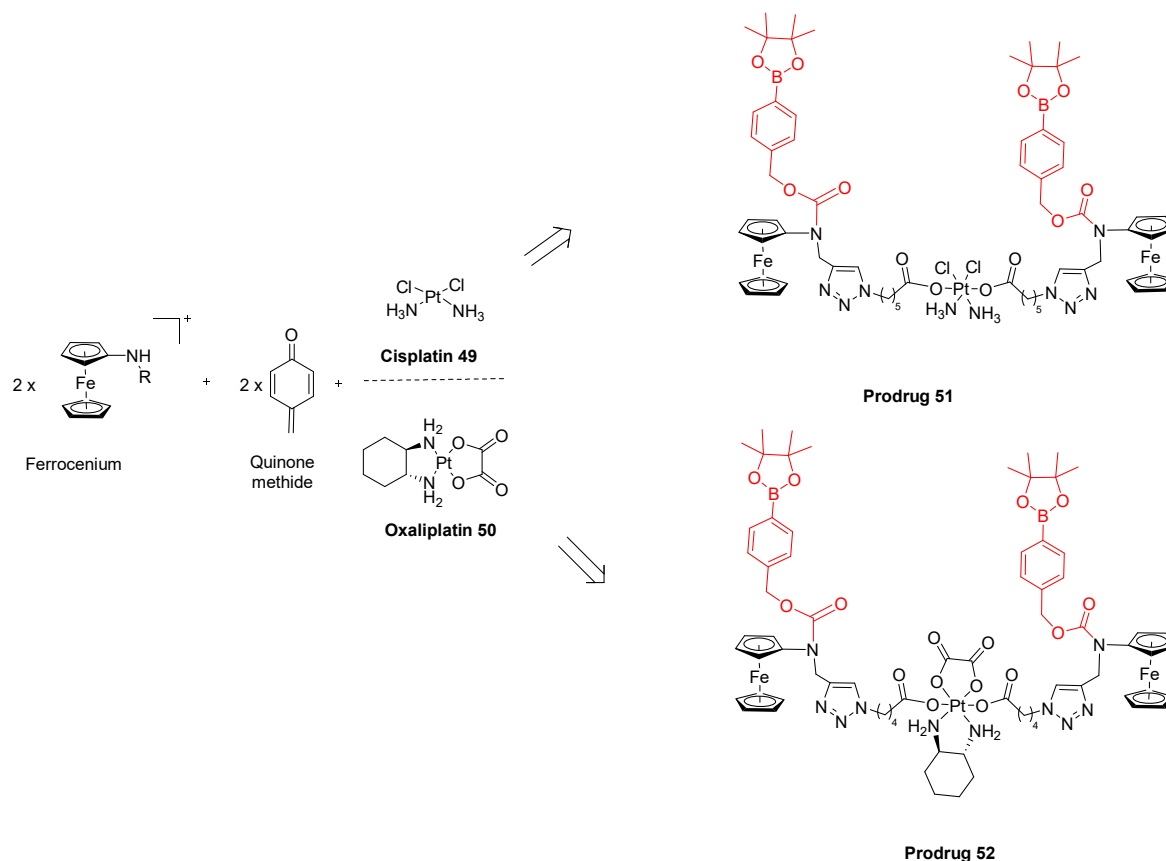
465 The authors further showed that the cytotoxicity was decreased when the ferrocene part was
 466 partly constituted of a cyclopentadiene carboxylic acid moiety.[71] Modification of the *N*-benzyl
 467 group by either introducing *ortho*- or *para*-substituent or replacement of the benzene ring by
 468 a pyridine nucleus was also counterproductive to the cytotoxicity on HL-60 cells.[71,72]
 469 Prodrug **44** was therefore selected for in vivo studies.[72,73] First, **44** was not toxic on healthy
 470 mice up to 6 mg/kg and **44** was further evaluated on L1210 leukemia xenografted mice. Six
 471 injections per day at 26 $\mu g/kg$ led to the extension of survival time (+ 30%) of the mice. The
 472 authors noted an increased oxidative stress in L1210 cancer cells recovered from treated
 473 animal.[72] Prodrug **44** was also evaluated on xenografts of human prostate adenocarcinoma
 474 in CBA mice in view of the high in vitro ROS production observed from prostate cancer cell
 475 lines. However, this latter in vivo assay showed a modest tumor mass reduction for the cohort
 476 treated with **44**.[73] Prodrug **44** was however described to aggregate in aqueous solution and
 477 new analogs were therefore designed in order to reduce this property. A *N*-propargyl prodrug
 478 **45** displaying lower hydrophobicity was indeed less susceptible to aggregation and was also
 479 shown to display in vitro cytotoxicity similar to that of **44**. Growth inhibition of Guerin's
 480 carcinoma in rat was observed when **45** was administrated intraperitoneally at a single dose
 481 of 30 mg/kg seven days after tumor transplantation.[74]

482 Aminoferrocene theranostic prodrugs (Scheme 16) were then developed by branching
 483 benzene boronate precursors of aminoferrocene to a [^{18}F]-fluoroglucose for positron emission
 484 tomography (PET).[75] Theranostic prodrug **46** had an in vitro cytotoxicity close to that of the
 485 reference prodrug **44** (e.g. against HL-60, $IC_{50}(\mathbf{46}) = 26 \mu M$ compared to $IC_{50}(\mathbf{44}) \sim 10 \mu M$).
 486 The corresponding free boronic acid of **46** was injected in mice bearing two tumors: PC3

487 (human prostate cancer) and AR42J (rat pancreatic cancer). PET analysis showed a moderate
488 localization of the tracer in both tumors but the measured radioactivity remain relatively stable
489 in the tumors for 60 minutes in comparison with the healthy organs of the mice.

490 An organic moiety able to target the lysosome was alternatively added on the benzene
491 boronate precursors of aminoferrocene.[76] The piperidine prodrug **47** (Scheme 16) was
492 prepared in order to obtain an ammonium form at physiological pH leading to lysosome
493 trapping and accumulation. Biophysical properties of **47** were compared to the reference
494 prodrug **44** and were shown significantly improved. In particular, the hydroxyl radical formation
495 was more efficient from prodrug **47** and this was transcribed with the higher in vitro cytotoxicity
496 observed for **47** than for **44** against several cancer cell lines (6 to 8 folds more active). The
497 ability of prodrug **47** to disrupt lysosomal function was confirmed by a fluorescence imaging
498 experiment. Prodrug **47** was evaluated in Nemeth-Kellner lymphoma xenograft mice model by
499 intraperitoneal injection of eight doses of 40 mg/kg every two days for 15 days. The tumor
500 weight of treated animals was reduced in comparison with the untreated cohort but the results
501 were very contrasted.

502 These aminoferrocene precursors were further complexified by the increment of a platinum-
503 based antineoplastic prodrug moiety (**48**, **51** and **52**) (Scheme 16 and 17).[77–79]



Scheme 17. Bis “aminoferrocene-platinum” prodrugs.

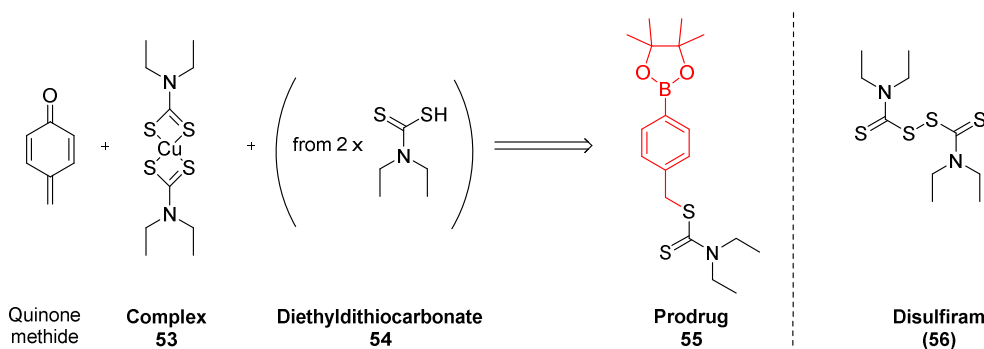
507 The bis “aminoferrocene-cisplatin” prodrug **51** was shown to effectively release cisplatin **49**
508 after addition of H₂O₂, indeed, the free aminoferrocenes generated are able to transfer one
509 electron that both reduces the metal complex into cisplatin and forms the activated
510 ferrocenium. **51** was evaluated against normal fibroblasts HDFa, ovarian carcinoma cell line
511 A2780 and the cisplatin resistant counterpart A2780cis cell line. Prodrug **51** was not toxic

512 against the healthy fibroblasts while activity of free cisplatin **49** was fully recovered when A2780
 513 cells were treated with **51** ($IC_{50} \sim 2 \mu M$). Interestingly, the resistant A2780cis cells behaved
 514 differently: activity of prodrug **51** ($IC_{50} = 6 \mu M$) was twice greater than cisplatin **49** ($IC_{50} = 13$
 515 μM). The authors revealed that prodrug **51** was not generating an aminoferrocene which
 516 strongly produces ROS but the activity of prodrug **51** was mostly due to the release of cisplatin
 517 **50** rather than the generally modest activity provided by ferrocenium. The oxaliplatin prodrug
 518 **52** was built with the same scaffold used for cisplatin prodrug **51** (Scheme 17).[78] In construct
 519 **52**, the spacer between the ferrocene and the platinum-based drug was truncated (C_4 in lieu
 520 of C_5) in order to facilitate the intramolecular electron transfer within these two moieties.
 521 Prodrug **52** was indeed more active than **51** against both ovarian cancer cell lines in vitro : IC_{50}
 522 (A2780) = $0.4 \mu M$ and IC_{50} (A2780cis) = $0.7 \mu M$. Analog **52** followed the trend described for
 523 prodrug **51** in view of the stronger activity (over free cisplatin **49**) displayed by the free drug
 524 oxaliplatin **50** : IC_{50} (A2780) = $0.9 \mu M$ and IC_{50} (A2780cis) = $3 \mu M$. The authors further
 525 synthesized a mono-“carboplatin-aminoferrocene” prodrug **48** (Scheme 16).[79] Accumulation
 526 of **48** in the mitochondria of A2780 cancer cells was demonstrated using the mitochondrial
 527 tracker rhodamine R123 and it was assumed that this uptake was due to the release of a
 528 delocalized lipophilic cation: the generated ferrocenium. In vitro activity of **48** was then
 529 determined against the three aforementioned cell lines and adopted the tendency observed
 530 for cisplatin prodrug **51** but to a weaker extent.

531

532 Diethyldithiocarbamate **54**

533 Diethyldithiocarbamate **54** is a metabolite of disulfiram **56**, a drug used in clinic to treat chronic
 534 alcoholism and recently, copper complex of diethyldithiocarbamate **53** was shown to have
 535 anticancer activity.[81] The formation of this complex **53** generates ROS in the cancer cells
 536 and the Pu group prepared a prodrug **55** capitalizing on the ROS amplification due to both
 537 formation of the latter complex and a quinone methide (Scheme 18).[82]



539

539 **Scheme 18.** Structures of disulfiram and the prodrug of diethyldithiocarbamate.

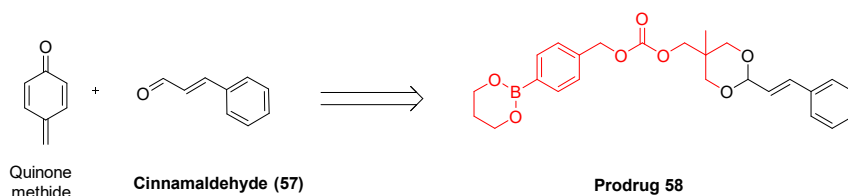
540

541 Prodrug **55** was tested against 4T1 breast cancer cells in vitro : In the presence of the nontoxic
 542 concentration of copper ($1 \mu M$), activity was six times more potent on cancer cells ($IC_{50} = 1$
 543 μM) than on normal fibroblasts NIH3T3 ($IC_{50} = 6 \mu M$). This difference of activity could be
 544 explained by the high ROS production of 4T1 which was essentially due to the
 545 diethyldithiocarbamate copper complex formation and minimally as a result of quinone methide
 546 generation. In vivo testing was made on a 4T1 xenograft mice and the most potent result was
 547 obtained using a co-injection of copper gluconate at 1.5 mg/kg with **55** at 37 mg/kg . Applying
 548 this protocol, a decrease of 80% of the tumors volume was observed in comparison to the
 549 inactive vehicle or copper gluconate alone.

550

551 Cinnamaldehyde **57**

552 Cinnamaldehyde **57** is a natural product found in cinnamon essential oil and used as food
553 flavoring. This aldehyde was shown to amplify ROS in cancer cells but this action is very limited
554 on healthy cells. Poor bioavailability of cinnamaldehyde **57** has prevented its application in
555 clinic and therefore this compound was a good candidate for prodrug development. Thus, the
556 Lee group has prepared a benzene boronate prodrug of cinnamaldehyde **58** (Scheme 19).[83]



557

558 **Scheme 19.** Prodrug of cinnamaldehyde.

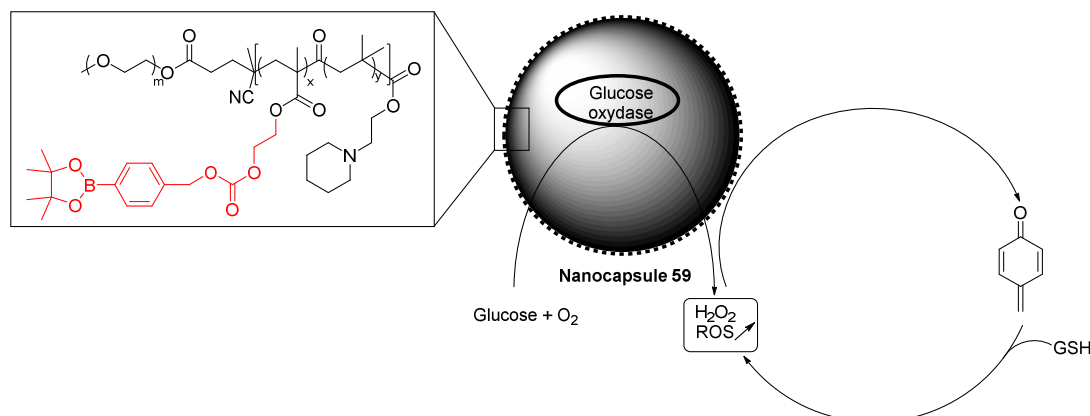
559

560 Under oxidative conditions, this prodrug **58** will generate a quinone methide able to covalently
561 trap antioxidants leading to ROS accumulation in cells. Moreover, a molecule of
562 cinnamaldehyde **57** will be released under acidic conditions found in cancer cells and then
563 enhanced the already high level of ROS. The authors first evaluated the ability of **58** to lower
564 the glutathione level in three cell lines: prostate cancer DU145, colon cancer SW620 and
565 fibroblasts NIH3T3. Only the DU145 cells were responsive to **58** and presented a reduction of
566 around 50% of intracellular glutathione concentration. Cytotoxicity of prodrug **58** was weak
567 against the three cell lines and DU145 cells were more affected ($IC_{50} = 48 \mu M$) than the NIH3T3
568 fibroblasts ($IC_{50} = 182 \mu M$). A tumor xenograft mouse model of DU145 cells was used to
569 evaluate the in vivo antitumor effect of **58** and camptothecin **21** as reference drug. Seven
570 injections every 3 days of either **58** or camptothecin **21** at 2 mg/kg showed the same tumor
571 volume reduction ($\sim 75\%$). Prodrug **58** was more active than control compound
572 cinnamaldehyde **57** or a quinone methide generator alone.

573

574 Glucose oxidase

575 The glucose oxidase enzyme catalyze the reaction of glucose and oxygen into gluconolactone
576 and hydrogen peroxide. This enzyme can therefore generate ROS from two compounds
577 naturally abundant in cells. To capitalize on this, Li et al.[84] have prepared nanocapsules **59**
578 able to entrap glucose oxidase (Scheme 20).



579

580 **Scheme 20.** Nanocapsules loaded with glucose oxidase for the amplification of ROS within
581 the tumor microenvironment.

582

583 The shell of the capsule was made of a diblock copolymer of PEG and polymethacrylate
584 grafted with benzene boronate and piperidine moieties. Protonation of piperidine in the acidic
585 tumor environment increases the permeability of the nanocapsule and allows the entry of
586 glucose which lead to the strong production of H₂O₂. This enhanced level of hydrogen peroxide
587 further reinforces the oxidation of the benzene boronate part into glutathione scavenger
588 quinone methide. The authors verified that this dual acting nanoconstruct was operational in
589 vitro by measuring H₂O₂ production and quinone methide formation. Mice bearing lung
590 carcinoma A549 were treated with nanocapsule **59** and showed complete inhibition of tumor
591 growth in comparison with either glucose oxidase or empty nanocapsule alone.

592

593 **3. Pharmacological relevance**

594

595 In this section, the strategy of boron-containing prodrugs responsive to oxidative stress is
596 discussed in regards to its potential to reach the market as effective cancer treatment. Indeed,
597 boronic acid/boronate prodrug have been largely evaluated in animal models but no clinical
598 trials have been started with any of these molecules so far.

599 Nonetheless, the potential of these constructs is strong considering that several drugs
600 containing a boronic acid function, are already on the market.[28,85] Moreover, the
601 development of boron-containing classical drug remains a dynamic area of research.[86] In
602 terms of drug delivery, the boronic acid function is particularly relevant since it allows facilitated
603 internalization in cancer cells.[87,88] The reversible formation of ester bonds between boronic
604 acid and the diol of saccharides ensure this membrane crossing. Precisely, high affinity
605 between boronic acids and the glycocalix of cancer cells lead to the selective uptake of the
606 molecules bearing this moiety.

607 Furthermore, to improve the strategy of the small-molecule prodrugs, the kinetic of prodrug
608 conversion must be considered. At the tumor site, activation of boron-containing prodrugs by
609 ROS can either occur extra- or intracellularly. As the system is not closed, the liberated drug
610 will then freely diffuse around the tumor ($\sim 10^{-3}$ mm³; a mass of around 1,000 cancer cells) and
611 that will influence the concentration profile of the drug. Scission of the prodrugs should arise
612 locally to preserve an efficient dose of the liberated drugs within the tumor. In view of the
613 diffusion coefficient of small molecules (10^{-10} m².s⁻¹) and considering the aforementioned tumor
614 volume, oxidation of precursors into drugs should last approximately 2 minutes in order to
615 maintain the concentration of the free drugs equal to that of the corresponding prodrugs. When
616 the prodrug conversion implies an additional self-immolative step, the complete process must
617 not exceed the latter duration.

618 The reaction of boron-containing prodrug with the ROS species is bimolecular and the rate will
619 therefore depend on the concentration of both reactants: $v = k[\text{prodrug}][\text{ROS}]$. The
620 concentration of the prodrug is mostly guided by the dose injected to the biologic system but
621 levels of peroxynitrite and hydrogen peroxide is dictated by the living organism. Specific
622 activation in the tumor microenvironment can occur since the concentrations of peroxynitrite
623 and hydrogen peroxide are strongly increased in comparison with healthy tissues. Cellular
624 concentration of peroxynitrite can reach 50-100 μM in pathological conditions whereas a basal

625 concentration of 0.1-1 μM was estimated in healthy cells.[89,90] Physiological hydrogen
626 peroxide is produced at a steady-state concentration of 0.1-1 μM which rises to 10-100 μM in
627 malignant organs.[91,92]

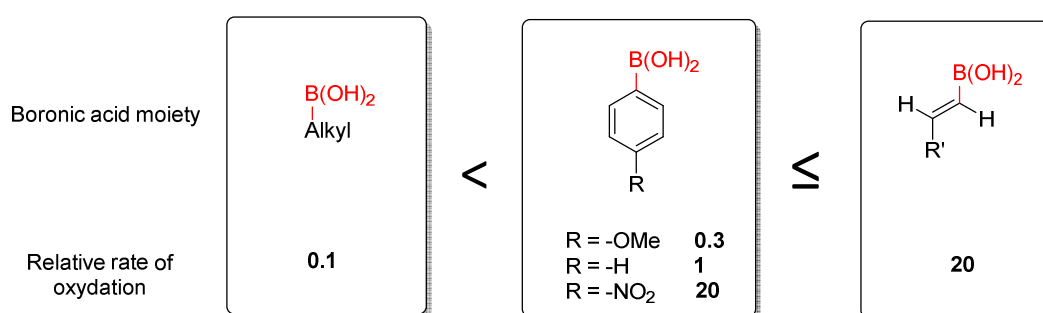
628 In this activation strategy, two parameters must be taken into account: the half-life of each
629 ROS in vivo and the rate constant associated to a ROS and a particular prodrug structure.

630 As mentioned earlier, at physiological pH, oxidation of the carbon-boron bond by peroxynitrite
631 is 10^6 faster than that obtained with hydrogen peroxide: e.g. conversion of phenylboronic acid
632 to phenol occurred with rate constant of $1 \times 10^6 \text{ M}^{-1} \cdot \text{s}^{-1}$ with peroxynitrite and approximately
633 $1\text{-}2 \text{ M}^{-1} \cdot \text{s}^{-1}$ with hydrogen peroxide.²⁵ In vivo, peroxynitrite has a half-life of ~ 10 ms and reacts
634 preponderantly but reversibly with carbon dioxide (1-2 mM) to form nitrosoperoxocarbonate
635 anion (ONOOCO_2^-) at a rate constant of $0.5 \times 10^5 \text{ M}^{-1} \cdot \text{s}^{-1}$. As opposed to hypochlorite anion
636 which react faster with biomolecules than boronate/boronic acid in vivo, peroxynitrite is able to
637 oxidize the carbon-boron bond due to the rapid kinetic of this reaction over the addition of
638 carbon dioxide.

639 In biological systems, hydrogen peroxide also reacts with biomolecules such as amino acids
640 and metals (free or inside metallo-enzymes). Consequently, its half-life in cells is ~ 1 ms. The
641 reaction with the thiol group of cysteine residues was described as the fastest physiological
642 transformation of hydrogen peroxide with a rate constant up to $10^6 \text{ M}^{-1} \cdot \text{s}^{-1}$. [93,94]

643 Given the differences of reactivity of both involved oxidative species, peroxynitrite is likely to
644 be the main actor for the conversion of these prodrugs into the corresponding free drugs. In
645 view of the short half-life of oxidative species, increasing the rate constant of this oxidation
646 reaction should result to a greater number of available peroxynitrite molecules that can react
647 with the boronic acid prodrug. This would lead to a better yield of prodrug transformation at the
648 tumor site and then improve the chance of treatment efficacy. Notably, the structure of the
649 prodrug will also greatly affect the kinetic of oxidation in regards of the ROS involved in the
650 reaction. The possibility of modulating the prodrug scaffold in favor of a faster reactivity toward
651 ROS is crucial and can be operated by medicinal chemists.

652 In term of structure-kinetic studies of boronic acids conversion into alcohols, we noted that
653 aliphatic boronic acids are 10 times slower than benzene boronic acids (Scheme 21). [25]



654

655 **Scheme 21.** Relative rate of C-B bonds oxidation of alkyl, benzyl and vinyl boronic acid
656 derivatives.

657

658 The oxidation kinetic of benzene boronic acids is dependent of the substitutions of the aromatic
659 nucleus.[24,30] Adding a strongly electron-withdrawing substituent such as a nitro group at the
660 *para* position of the ring increased the oxidation rate by 20-fold whereas an electron-donating
661 methoxy group at the same position divided this rate by a factor of three. Although electron-
662 withdrawing group substitution of the benzenic ring lead to a faster formation of the quinone

663 methide intermediate, this latter modification also cause a dramatic reduction of the kinetic of
664 the following self-immolation step.[32] Therefore, no substitution of benzene boronate nucleus
665 as self-immolative promoiety can be envisioned to increase the global rate of the
666 oxidation/disassembly steps of such constructs.

667 The vinyl boronic acid group was also shown to release an effector through oxidation and
668 subsequent self-immolation process.[30,31,95] The oxidation of the vinyl boronic acid motif was
669 20 times more rapid than that of the equivalent unsubstituted benzene boronic acid group.[30]
670 This difference of reactivity could be attributed to a faster self-immolation step since the π
671 electrons of the double bond are not delocalized within a benzene nucleus and therefore
672 available for the elimination reaction. Moreover, the empty p-orbital of the boron in vinyl boronic
673 acid motif is less hindered than in the benzenic equivalent leading to an easiest access of the
674 nucleophilic oxidative species. Eventually, this motif could be further engineered to potentially
675 increase the global rate of effector release.

676 With the condition that an average drug concentration of 10 μM is required within the tumor of
677 around 10^{-3} mm^3 , the rate of the reaction ($v = k[\text{prodrug}][\text{ROS}]$) should not fall below 10 μM
678 per 2 minutes which is about $0.1 \mu\text{M}\cdot\text{s}^{-1}$ (total conversion inside the tumor). Given the
679 concentration of peroxynitrite ($\sim 10 \mu\text{M}$; the most reactive ROS) in cancer cells, only prodrugs
680 oxidized at rate constant (k) higher than $10^3 \text{ M}^{-1}\cdot\text{s}^{-1}$ would be effective. Nonetheless, due to the
681 short half-life of peroxynitrite ($\sim 10 \text{ ms}$), we estimate that the reaction of the latter oxidant with
682 a particular boronic acid prodrug should react at a rate constant superior to $10^7 \text{ M}^{-1}\cdot\text{s}^{-1}$ in order
683 to afford 10 μM of drug localized at the tumor site. In light of this short physiological half-life,
684 targeting mitochondria is a relevant strategy in order to efficiently reach the cellular ROS. Such
685 vectorized prodrug containing a delocalized lipophilic cation was already developed by the
686 Mokhir group.[79]

687 In regards of the aforementioned boronic acid promoieties, we noticed that the quinone
688 methide species generated from benzene boronates were not strongly cytotoxic but very
689 efficient at scavenging antioxidants.[44,70,83,84] Remarkably, it was occasionally reported
690 that the boronic promoiety was not completely masking the pharmacological activity of the
691 branched drug.^{45,60} This suggests that the attachment of a benzene boronic acid promoiety to
692 a drug do not provoke the automatic discontinuation of the bioactivity. Furthermore, the
693 nominal boronic acid function is often used in this reviewed prodrug strategy and it was recently
694 proposed that the latter function could be used as a bioisoster of a hydroxyl group. Some
695 successful drug analogs were indeed developed by the Wang group[96–98] that formerly
696 developed boronic acid-containing prodrugs (vide supra).

697 The same group showed that boronic acid prodrug were also activated by the cytochromes
698 P450.[42] Thus, the benzene boronic promoiety could even be employed for the development
699 of several types of prodrug allowing the prolonged release of any drug for the treatment of any
700 disease.[99] Consequently, this activation could compete with the expected oxidation by the
701 ROS of cancer-targeting boronic acid prodrugs within the tumor microenvironment. It is
702 important to note, however, that unlike a direct chemical reaction between an oxidant and a
703 boronic acid molecule, the reaction of the latter function with the cytochromes P450 is an
704 enzymatic reaction. This implies the entrance of the prodrug into the active site before oxidation
705 of the C-B bond. In order to develop boronic acid prodrugs specifically targeting tumors, their
706 oxidation by cytochromes P450 should be evaluated. In case of unwanted interaction,
707 modulation of the structural core of the boronic acid promoiety should be therefore considered
708 to impede the prodrug access to the catalytic sites of the cytochromes P450.

709

4. Conclusion

710
711

712 This review reports on the different small-molecule, polymeric and nanoparticle-based
713 prodrugs activated through oxidation of intrinsic carbon-boron bonds by ROS from tumor
714 environment. The literature reveals several constructs with interesting activity and until now,
715 none of these prodrugs have entered into clinical trial. In view of the in vivo data, this prodrug
716 strategy is promising for the treatment of several tumors such as leukemia, breast and
717 pancreatic cancers which produce high concentrations of ROS. Chemical system leading to
718 both ROS amplification and anticancer agent delivery were particularly effective. In order to
719 obtain a ROS-activated boronic acid prodrug with a great therapeutic potential, it would be
720 beneficial to develop a structure which could both intensify the ROS level within cancer cells
721 and ensure rapid release of a drug by virtue of a rapid C-B oxidation.

722

ACKNOWLEDGMENTS

723

724 H. Maslah is supported by the “Ministère de l'Education Nationale de la Recherche et de la
725 Technologie”. This work was funded by the “Ligue Nationale Contre le Cancer” (comité de
726 l'Essonne) and the “Fondation ARC pour la recherche sur le cancer”. C. Skarbek is financed
727 by a postdoctoral training grant from the “Fondation ARC pour la recherche sur le cancer”.

728

REFERENCES

729

730

- 731 [1] A. Albert, Chemical Aspects of Selective Toxicity, *Nature*. 182 (1958) 421–423.
732 <https://doi.org/10.1038/182421a0>.
- 733 [2] J. Rautio, H. Kumpulainen, T. Heimbach, R. Oliyai, D. Oh, T. Järvinen, J. Savolainen,
734 Prodrugs: design and clinical applications, *Nat Rev Drug Discov*. 7 (2008) 255–270.
735 <https://doi.org/10.1038/nrd2468>.
- 736 [3] K.M. Huttunen, H. Raunio, J. Rautio, Prodrugs--from serendipity to rational design,
737 *Pharmacological Reviews*. 63 (2011) 750–71. <https://doi.org/10.1124/pr.110.003459>.
- 738 [4] J. Rautio, N.A. Meanwell, L. Di, M.J. Hageman, The expanding role of prodrugs in
739 contemporary drug design and development, *Nature Reviews. Drug Discovery*. 17
740 (2018) 559–587. <https://doi.org/10.1038/nrd.2018.46>.
- 741 [5] W.A. Denny, Prodrug strategies in cancer therapy, *European Journal of Medicinal*
742 *Chemistry*. 36 (2001) 577–95. [https://doi.org/10.1016/s0223-5234\(01\)01253-3](https://doi.org/10.1016/s0223-5234(01)01253-3).
- 743 [6] X. Zhang, X. Li, Q. You, X. Zhang, Prodrug strategy for cancer cell-specific targeting: A
744 recent overview, *European Journal of Medicinal Chemistry*. 139 (2017) 542–563.
745 <https://doi.org/10.1016/j.ejmech.2017.08.010>.
- 746 [7] V. Taresco, C. Alexander, N. Singh, A.K. Pearce, Stimuli-Responsive Prodrug
747 Chemistries for Drug Delivery, *Adv Ther-Germany*. 1 (2018) 1800030.
748 <https://doi.org/10.1002/Adtp.201800030>.
- 749 [8] L. Bildstein, C. Dubernet, P. Couvreur, Prodrug-based intracellular delivery of
750 anticancer agents, *Advanced Drug Delivery Reviews*. 63 (2011) 3–23.
751 <https://doi.org/10.1016/j.addr.2010.12.005>.
- 752 [9] R. Walther, J. Rautio, A.N. Zelikin, Prodrugs in medicinal chemistry and enzyme
753 prodrug therapies, *Advanced Drug Delivery Reviews*. 118 (2017) 65–77.
754 <https://doi.org/10.1016/j.addr.2017.06.013>.

- 755 [10] Y. Hamada, Recent progress in prodrug design strategies based on generally
756 applicable modifications, *Bioorganic & Medicinal Chemistry Letters*. 27 (2017) 1627–
757 1632. <https://doi.org/10.1016/j.bmcl.2017.02.075>.
- 758 [11] J.M. Brown, W.R. Wilson, Exploiting tumour hypoxia in cancer treatment, *Nature*
759 *Reviews. Cancer*. 4 (2004) 437–47. <https://doi.org/10.1038/nrc1367>.
- 760 [12] W.R. Wilson, M.P. Hay, Targeting hypoxia in cancer therapy, *Nature Reviews. Cancer*.
761 11 (2011) 393–410. <https://doi.org/10.1038/nrc3064>.
- 762 [13] A. Sharma, J.F. Arambula, S. Koo, R. Kumar, H. Singh, J.L. Sessler, J.S. Kim, Hypoxia-
763 targeted drug delivery, *Chemical Society Reviews*. 48 (2019) 771–813.
764 <https://doi.org/10.1039/c8cs00304a>.
- 765 [14] D. Trachootham, J. Alexandre, P. Huang, Targeting cancer cells by ROS-mediated
766 mechanisms: a radical therapeutic approach?, *Nature Reviews. Drug Discovery*. 8
767 (2009) 579–91. <https://doi.org/10.1038/nrd2803>.
- 768 [15] K.-C. Yan, A.C. Sedgwick, Y. Zang, G.-R. Chen, X.-P. He, J. Li, J. Yoon, T.D. James,
769 Sensors, Imaging Agents, and Theranostics to Help Understand and Treat Reactive
770 Oxygen Species Related Diseases, *Small Methods*. 3 (2019) 1900013.
771 <https://doi.org/10.1002/smt.201900013>.
- 772 [16] G.Y. Liou, P. Storz, Reactive oxygen species in cancer, *Free Radical Research*. 44
773 (2010) 479–96. <https://doi.org/10.3109/10715761003667554>.
- 774 [17] H.Y. Tan, N. Wang, The Reactive Oxygen Species in Macrophage Polarization:
775 Reflecting Its Dual Role in Progression and Treatment of Human Diseases, 2016 (2016)
776 2795090. <https://doi.org/10.1155/2016/2795090>.
- 777 [18] B.Z. Qian, J.W. Pollard, Macrophage diversity enhances tumor progression and
778 metastasis, *Cell*. 141 (2010) 39–51. <https://doi.org/10.1016/j.cell.2010.03.014>.
- 779 [19] X. Peng, V. Gandhi, ROS-activated anticancer prodrugs: a new strategy for tumor-
780 specific damage, *Therapeutic Delivery*. 3 (2012) 823–33.
781 <https://doi.org/10.4155/tde.12.61>.
- 782 [20] J. Peiró Cadahía, V. Previtali, Prodrug strategies for targeted therapy triggered by
783 reactive oxygen species, 10 (2019) 1531–1549. <https://doi.org/10.1039/c9md00169g>.
- 784 [21] H. Ye, Y. Zhou, X. Liu, Y. Chen, S. Duan, R. Zhu, Y. Liu, Recent Advances on Reactive
785 Oxygen Species-Responsive Delivery and Diagnosis System, 20 (2019) 2441–2463.
786 <https://doi.org/10.1021/acs.biomac.9b00628>.
- 787 [22] J.P.M. Antonio, R. Russo, C.P. Carvalho, P. Cal, P.M.P. Gois, Boronic acids as building
788 blocks for the construction of therapeutically useful bioconjugates, *Chemical Society*
789 *Reviews*. 48 (2019) 3513–3536. <https://doi.org/10.1039/c9cs00184k>.
- 790 [23] D. Andina, J.C. Leroux, P. Luciani, Ratiometric Fluorescent Probes for the Detection of
791 Reactive Oxygen Species, *Chemistry*. 23 (2017) 13549–13573.
792 <https://doi.org/10.1002/chem.201702458>.
- 793 [24] S. Cao, R. Christiansen, X. Peng, Substituent effects on oxidation-induced formation of
794 quinone methides from arylboronic ester precursors, *Chemistry (Weinheim an Der*
795 *Bergstrasse, Germany)*. 19 (2013) 9050–8. <https://doi.org/10.1002/chem.201300539>.
- 796 [25] J. Zielonka, A. Sikora, M. Hardy, J. Joseph, B.P. Dranka, B. Kalyanaraman, Boronate
797 probes as diagnostic tools for real time monitoring of peroxynitrite and hydroperoxides,
798 *Chemical Research in Toxicology*. 25 (2012) 1793–9. <https://doi.org/10.1021/tx300164j>.
- 799 [26] A. Sikora, J. Zielonka, M. Lopez, J. Joseph, B. Kalyanaraman, Direct oxidation of
800 boronates by peroxynitrite: mechanism and implications in fluorescence imaging of
801 peroxynitrite, *Free Radical Biology & Medicine*. 47 (2009) 1401–7.
802 <https://doi.org/10.1016/j.freeradbiomed.2009.08.006>.
- 803 [27] A. Sikora, J. Zielonka, M. Lopez, A. Dybala-Defratyka, J. Joseph, A. Marcinek, B.
804 Kalyanaraman, Reaction between peroxynitrite and boronates: EPR spin-trapping,
805 HPLC Analyses, and quantum mechanical study of the free radical pathway, *Chemical*
806 *Research in Toxicology*. 24 (2011) 687–97. <https://doi.org/10.1021/tx100439a>.
- 807 [28] S.J. Baker, C.Z. Ding, T. Akama, Y.K. Zhang, V. Hernandez, Y. Xia, Therapeutic
808 potential of boron-containing compounds, *Future Medicinal Chemistry*. 1 (2009) 1275–
809 88. <https://doi.org/10.4155/fmc.09.71>.

- 810 [29] R.D. Hanna, Y. Naro, A. Deiters, P.E. Floreancig, Alcohol, Aldehyde, and Ketone
811 Liberation and Intracellular Cargo Release through Peroxide-Mediated α -Boryl Ether
812 Fragmentation, *Journal of the American Chemical Society*. 138 (2016) 13353–13360.
813 <https://doi.org/10.1021/jacs.6b07890>.
- 814 [30] R.A. Mosey, P.E. Floreancig, Versatile approach to α -alkoxy carbamate synthesis and
815 stimulus-responsive alcohol release, *Organic & Biomolecular Chemistry*. 10 (2012)
816 7980–5. <https://doi.org/10.1039/c2ob26571k>.
- 817 [31] A.D. Brooks, H. Mohapatra, S.T. Phillips, Design, Synthesis, and Characterization of
818 Small-Molecule Reagents That Cooperatively Provide Dual Readouts for Triaging and,
819 When Necessary, Quantifying Point-of-Need Enzyme Assays, *The Journal of Organic*
820 *Chemistry*. 80 (2015) 10437–45. <https://doi.org/10.1021/acs.joc.5b02013>.
- 821 [32] A. Alouane, R. Labruere, T. Le Saux, F. Schmidt, L. Jullien, Self-immolative spacers:
822 kinetic aspects, structure-property relationships, and applications, *Angewandte Chemie*.
823 54 (2015) 7492–509. <https://doi.org/10.1002/anie.201500088>.
- 824 [33] M. Gisbert-Garzarán, M. Manzano, M. Vallet-Regí, Self-immolative chemistry in
825 nanomedicine, *Chemical Engineering Journal*. 340 (2018) 24–31.
826 <https://doi.org/10.1016/j.cej.2017.12.098>.
- 827 [34] H.K. Patel, T. Bihani, Selective estrogen receptor modulators (SERMs) and selective
828 estrogen receptor degraders (SERDs) in cancer treatment, *Pharmacology &*
829 *Therapeutics*. 186 (2018) 1–24. <https://doi.org/10.1016/j.pharmthera.2017.12.012>.
- 830 [35] Q. Jiang, Q. Zhong, Q. Zhang, S. Zheng, G. Wang, Boron-Based 4-Hydroxytamoxifen
831 Bioisosteres for Treatment of de Novo Tamoxifen Resistant Breast Cancer, *ACS*
832 *Medicinal Chemistry Letters*. 3 (2012) 392–396. <https://doi.org/10.1021/ml3000287>.
- 833 [36] C. Zhang, Q. Zhong, Q. Zhang, S. Zheng, L. Miele, G. Wang, Boronic prodrug of
834 endoxifen as an effective hormone therapy for breast cancer, *Breast Cancer Research*
835 *and Treatment*. 152 (2015) 283–91. <https://doi.org/10.1007/s10549-015-3461-9>.
- 836 [37] Q. Zhong, C. Zhang, Q. Zhang, L. Miele, S. Zheng, G. Wang, Boronic prodrug of 4-
837 hydroxytamoxifen is more efficacious than tamoxifen with enhanced bioavailability
838 independent of CYP2D6 status, *BMC Cancer*. 15 (2015) 625.
839 <https://doi.org/10.1186/s12885-015-1621-2>.
- 840 [38] M. Manal, M.J. Chandrasekar, J. Gomathi Priya, M.J. Nanjan, Inhibitors of histone
841 deacetylase as antitumor agents: A critical review, *Bioorganic Chemistry*. 67 (2016) 18–
842 42. <https://doi.org/10.1016/j.bioorg.2016.05.005>.
- 843 [39] Y. Liao, L. Xu, S. Ou, H. Edwards, D. Luedtke, Y. Ge, Z. Qin, H₂O₂/Peroxynitrite-
844 Activated Hydroxamic Acid HDAC Inhibitor Prodrugs Show Antileukemic Activities
845 against AML Cells, *ACS Medicinal Chemistry Letters*. 9 (2018) 635–640.
846 <https://doi.org/10.1021/acsmedchemlett.8b00057>.
- 847 [40] S. Zheng, S. Guo, Q. Zhong, C. Zhang, J. Liu, L. Yang, Q. Zhang, G. Wang,
848 Biocompatible Boron-Containing Prodrugs of Belinostat for the Potential Treatment of
849 Solid Tumors, *ACS Medicinal Chemistry Letters*. 9 (2018) 149–154.
850 <https://doi.org/10.1021/acsmedchemlett.7b00504>.
- 851 [41] P.S. Hole, J. Zabkiewicz, C. Munje, Z. Newton, L. Pearn, P. White, N. Marquez, R.K.
852 Hills, A.K. Burnett, A. Tonks, R.L. Darley, Overproduction of NOX-derived ROS in AML
853 promotes proliferation and is associated with defective oxidative stress signaling, *Blood*.
854 122 (2013) 3322–30. <https://doi.org/10.1182/blood-2013-04-491944>.
- 855 [42] C. Zhang, S. Guo, Q. Zhong, Q. Zhang, A. Hossain, S. Zheng, Metabolism and
856 Pharmacokinetic Study of the Boron-Containing Prodrug of Belinostat (ZL277), a Pan
857 HDAC Inhibitor with Enhanced Bioavailability, 12 (2019).
858 <https://doi.org/10.3390/ph12040180>.
- 859 [43] R.A. Varier, H.T. Timmers, Histone lysine methylation and demethylation pathways in
860 cancer, *Biochimica et Biophysica Acta*. 1815 (2011) 75–89.
861 <https://doi.org/10.1016/j.bbcan.2010.10.002>.
- 862 [44] M. Engel, Y.S. Gee, Novel dual-action prodrug triggers apoptosis in glioblastoma cells
863 by releasing a glutathione quencher and lysine-specific histone demethylase 1A
864 inhibitor, 149 (2019) 535–550. <https://doi.org/10.1111/jnc.14655>.

- 865 [45] B. Bielec, I. Poetsch, E. Ahmed, P. Heffeter, B.K. Keppler, C.R. Kowol, Reactive
866 Oxygen Species (ROS)-Sensitive Prodrugs of the Tyrosine Kinase Inhibitor Crizotinib,
867 *Molecules*. 25 (2020). <https://doi.org/10.3390/molecules25051149>.
- 868 [46] J. Peiró Cadahía, J. Bondebjerg, C.A. Hansen, V. Previtali, A.E. Hansen, T.L.
869 Andresen, M.H. Clausen, Synthesis and Evaluation of Hydrogen Peroxide Sensitive
870 Prodrugs of Methotrexate and Aminopterin for the Treatment of Rheumatoid Arthritis, 61
871 (2018) 3503–3515. <https://doi.org/10.1021/acs.jmedchem.7b01775>.
- 872 [47] V. Previtali, K. Petrovic, J. Peiró Cadahía, N.S. Troelsen, M.H. Clausen, Auxiliary in
873 vitro and in vivo biological evaluation of hydrogen peroxide sensitive prodrugs of
874 methotrexate and aminopterin for the treatment of rheumatoid arthritis, *Bioorganic &*
875 *Medicinal Chemistry*. 28 (2020) 115247. <https://doi.org/10.1016/j.bmc.2019.115247>.
- 876 [48] Y. Ai, O.N. Obianom, M. Kuser, Y. Li, Y. Shu, F. Xue, Enhanced Tumor Selectivity of 5-
877 Fluorouracil Using a Reactive Oxygen Species-Activated Prodrug Approach, *ACS*
878 *Medicinal Chemistry Letters*. 10 (2019) 127–131.
879 <https://doi.org/10.1021/acsmedchemlett.8b00539>.
- 880 [49] K. Matsushita, T. Okuda, A Hydrogen Peroxide Activatable Gemcitabine Prodrug for the
881 Selective Treatment of Pancreatic Ductal Adenocarcinoma, 14 (2019) 1384–1391.
882 <https://doi.org/10.1002/cmdc.201900324>.
- 883 [50] M.L. Rothenberg, Irinotecan (CPT-11): recent developments and future directions--
884 colorectal cancer and beyond, *The Oncologist*. 6 (2001) 66–80.
885 <https://doi.org/10.1634/theoncologist.6-1-66>.
- 886 [51] L. Wang, S. Xie, L. Ma, Y. Chen, W. Lu, 10-Boronic acid substituted camptothecin as
887 prodrug of SN-38, *European Journal of Medicinal Chemistry*. 116 (2016) 84–89.
888 <https://doi.org/10.1016/j.ejmech.2016.03.063>.
- 889 [52] E.J. Kim, S. Bhuniya, H. Lee, H.M. Kim, C. Cheong, S. Maiti, K.S. Hong, J.S. Kim, An
890 activatable prodrug for the treatment of metastatic tumors, *Journal of the American*
891 *Chemical Society*. 136 (2014) 13888–94. <https://doi.org/10.1021/ja5077684>.
- 892 [53] O. Redy-Keisar, S. Ferber, R. Satchi-Fainaro, D. Shabat, NIR Fluorogenic Dye as a
893 Modular Platform for Prodrug Assembly: Real-Time in vivo Monitoring of Drug Release,
894 *ChemMedChem*. 10 (2015) 999–1007. <https://doi.org/10.1002/cmdc.201500060>.
- 895 [54] Y. Octavia, C.G. Tocchetti, K.L. Gabrielson, S. Janssens, H.J. Crijns, A.L. Moens,
896 Doxorubicin-induced cardiomyopathy: from molecular mechanisms to therapeutic
897 strategies, *Journal of Molecular and Cellular Cardiology*. 52 (2012) 1213–25.
898 <https://doi.org/10.1016/j.yjmcc.2012.03.006>.
- 899 [55] C. Skarbek, S. Serra, H. Maslah, E. Rascol, R. Labruère, Arylboronate prodrugs of
900 doxorubicin as promising chemotherapy for pancreatic cancer, *Bioorganic Chemistry*.
901 91 (2019) 103158. <https://doi.org/10.1016/j.bioorg.2019.103158>.
- 902 [56] M. Ye, Y. Han, J. Tang, Y. Piao, X. Liu, Z. Zhou, J. Gao, J. Rao, Y. Shen, A Tumor-
903 Specific Cascade Amplification Drug Release Nanoparticle for Overcoming Multidrug
904 Resistance in Cancers, *Advanced Materials (Deerfield Beach, Fla.)*. 29 (2017).
905 <https://doi.org/10.1002/adma.201702342>.
- 906 [57] X. Gao, J. Cao, Y. Song, X. Shu, J. Liu, J.Z. Sun, B. Liu, B.Z. Tang, A unimolecular
907 theranostic system with H₂O₂-specific response and AIE-activity for doxorubicin
908 releasing and real-time tracking in living cells, *RSC Advances*. 8 (2018) 10975–10979.
909 <https://doi.org/10.1039/C8RA01185K>.
- 910 [58] Y. Xu, W. Shi, H₂O₂-Responsive Organosilica-Doxorubicin Nanoparticles for
911 Targeted Imaging and Killing of Cancer Cells Based on a Synthesized Silane-Borate
912 Precursor, 14 (2019) 1079–1085. <https://doi.org/10.1002/cmdc.201900142>.
- 913 [59] M.V. Blagosklonny, T. Fojo, Molecular effects of paclitaxel: myths and reality (a critical
914 review), *International Journal of Cancer*. 83 (1999) 151–6.
915 [https://doi.org/10.1002/\(sici\)1097-0215\(19991008\)83:2<151::aid-ijc1>3.0.co;2-5](https://doi.org/10.1002/(sici)1097-0215(19991008)83:2<151::aid-ijc1>3.0.co;2-5).
- 916 [60] C. Dong, Q. Zhou, J. Xiang, F. Liu, Z. Zhou, Y. Shen, Self-assembly of oxidation-
917 responsive polyethylene glycol-paclitaxel prodrug for cancer chemotherapy, *Journal of*
918 *Controlled Release : Official Journal of the Controlled Release Society*. 321 (2020) 529–
919 539. <https://doi.org/10.1016/j.jconrel.2020.02.038>.

- 920 [61] G. Ravikumar, M. Bagheri, D.K. Saini, H. Chakrapani, A small molecule for theraNOstic
921 targeting of cancer cells, *Chemical Communications (Cambridge, England)*. 53 (2017)
922 13352–13355. <https://doi.org/10.1039/c7cc08526e>.
- 923 [62] Y. Kuang, K. Balakrishnan, V. Gandhi, X. Peng, Hydrogen peroxide inducible DNA
924 cross-linking agents: targeted anticancer prodrugs, *Journal of the American Chemical*
925 *Society*. 133 (2011) 19278–81. <https://doi.org/10.1021/ja2073824>.
- 926 [63] M. Li, S. Li, H. Chen, R. Hu, L. Liu, F. Lv, S. Wang, Preparation of Conjugated Polymer
927 Grafted with H₂O₂-Sensitive Prodrug for Cell Imaging and Tumor Cell Killing, *ACS*
928 *Applied Materials & Interfaces*. 8 (2016) 42–6. <https://doi.org/10.1021/acsami.5b11846>.
- 929 [64] W. Chen, Y. Han, X. Peng, Aromatic Nitrogen Mustard-Based Prodrugs: Activity,
930 Selectivity, and the Mechanism of DNA Cross-Linking, *Chemistry – A European*
931 *Journal*. 20 (2014) 7410–7418. <https://doi.org/10.1002/chem.201400090>.
- 932 [65] W. Chen, K. Balakrishnan, Y. Kuang, Y. Han, M. Fu, V. Gandhi, X. Peng, Reactive
933 oxygen species (ROS) inducible DNA cross-linking agents and their effect on cancer
934 cells and normal lymphocytes, *Journal of Medicinal Chemistry*. 57 (2014) 4498–510.
935 <https://doi.org/10.1021/jm401349g>.
- 936 [66] W. Chen, H. Fan, K. Balakrishnan, Y. Wang, H. Sun, Y. Fan, V. Gandhi, L.A. Arnold,
937 Discovery and Optimization of Novel Hydrogen Peroxide Activated Aromatic Nitrogen
938 Mustard Derivatives as Highly Potent Anticancer Agents, 61 (2018) 9132–9145.
939 <https://doi.org/10.1021/acs.jmedchem.8b00559>.
- 940 [67] S. Cao, Y. Wang, X. Peng, ROS-inducible DNA cross-linking agent as a new anticancer
941 prodrug building block, *Chemistry (Weinheim an Der Bergstrasse, Germany)*. 18 (2012)
942 3850–4. <https://doi.org/10.1002/chem.201200075>.
- 943 [68] S. Cao, Y. Wang, X. Peng, The leaving group strongly affects H₂O₂-induced DNA cross-
944 linking by arylboronates, *The Journal of Organic Chemistry*. 79 (2014) 501–8.
945 <https://doi.org/10.1021/jo401901x>.
- 946 [69] Y. Wang, H. Fan, K. Balakrishnan, Z. Lin, S. Cao, W. Chen, Y. Fan, Q.A. Guthrie, H.
947 Sun, K.A. Teske, V. Gandhi, L.A. Arnold, X. Peng, Hydrogen peroxide activated
948 quinone methide precursors with enhanced DNA cross-linking capability and cytotoxicity
949 towards cancer cells, *European Journal of Medicinal Chemistry*. 133 (2017) 197–207.
950 <https://doi.org/10.1016/j.ejmech.2017.03.041>.
- 951 [70] H. Hagen, P. Marzenell, E. Jentzsch, F. Wenz, M.R. Veldwijk, A. Mokhir,
952 Aminoferrocene-based prodrugs activated by reactive oxygen species, *Journal of*
953 *Medicinal Chemistry*. 55 (2012) 924–34. <https://doi.org/10.1021/jm2014937>.
- 954 [71] P. Marzenell, H. Hagen, L. Sellner, T. Zenz, R. Grinyte, V. Pavlov, S. Daum, A. Mokhir,
955 Aminoferrocene-based prodrugs and their effects on human normal and cancer cells as
956 well as bacterial cells, *Journal of Medicinal Chemistry*. 56 (2013) 6935–44.
957 <https://doi.org/10.1021/jm400754c>.
- 958 [72] S. Daum, V.F. Chekhun, I.N. Todor, N.Y. Lukianova, Y.V. Shvets, L. Sellner, K. Putzker,
959 J. Lewis, T. Zenz, I.A. de Graaf, G.M. Groothuis, A. Casini, O. Zozulia, F. Hampel, A.
960 Mokhir, Improved synthesis of N-benzylaminoferrocene-based prodrugs and evaluation
961 of their toxicity and antileukemic activity, *Journal of Medicinal Chemistry*. 58 (2015)
962 2015–24. <https://doi.org/10.1021/jm5019548>.
- 963 [73] M. Schikora, A. Reznikov, L. Chaykovskaya, O. Sachinska, L. Polyakova, A. Mokhir,
964 Activity of aminoferrocene-based prodrugs against prostate cancer, *Bioorganic &*
965 *Medicinal Chemistry Letters*. 25 (2015) 3447–50.
966 <https://doi.org/10.1016/j.bmcl.2015.07.013>.
- 967 [74] S. Daum, S. Babiy, H. Konovalova, W. Hofer, A. Shtemenko, N. Shtemenko, C. Janko,
968 C. Alexiou, A. Mokhir, Tuning the structure of aminoferrocene-based anticancer
969 prodrugs to prevent their aggregation in aqueous solution, *Journal of Inorganic*
970 *Biochemistry*. 178 (2018) 9–17. <https://doi.org/10.1016/j.jinorgbio.2017.08.038>.
- 971 [75] S. Daum, J. Toms, V. Reshetnikov, H.G. Özkan, F. Hampel, S. Maschauer, A.
972 Hakimoun, F. Beierlein, L. Sellner, M. Schmitt, O. Prante, Identification of Boronic Acid
973 Derivatives as an Active Form of N-Alkylaminoferrocene-Based Anticancer Prodrugs

- 974 and Their Radiolabeling with (18)F, 30 (2019) 1077–1086.
975 <https://doi.org/10.1021/acs.bioconjchem.9b00019>.
- 976 [76] S. Daum, M.S.V. Reshetnikov, M. Sisa, T. Dumych, M.D. Lootsik, R. Bilyy, E. Bila, C.
977 Janko, C. Alexiou, M. Herrmann, L. Sellner, A. Mokhir, Lysosome-Targeting Amplifiers
978 of Reactive Oxygen Species as Anticancer Prodrugs, *Angewandte Chemie International*
979 *Edition*. 56 (2017) 15545–15549. <https://doi.org/10.1002/anie.201706585>.
- 980 [77] V. Reshetnikov, S. Daum, A. Mokhir, Cancer-Specific, Intracellular, Reductive Activation
981 of Anticancer Pt(IV) Prodrugs, *Chemistry (Weinheim an Der Bergstrasse, Germany)*. 23
982 (2017) 5678–5681. <https://doi.org/10.1002/chem.201701192>.
- 983 [78] V. Reshetnikov, A. Arkhypov, P.R. Julakanti, A. Mokhir, A cancer specific oxaliplatin-
984 releasing Pt(iv)-prodrug, *Dalton Transactions (Cambridge, England : 2003)*. 47 (2018)
985 6679–6682. <https://doi.org/10.1039/c8dt01458b>.
- 986 [79] V. Reshetnikov, S. Daum, C. Janko, W. Karawacka, R. Tietze, C. Alexiou, S. Paryzhak,
987 T. Dumych, R. Bilyy, P. Tripal, B. Schmid, R. Palmisano, A. Mokhir, ROS-Responsive
988 N-Alkylaminoferrocenes for Cancer-Cell-Specific Targeting of Mitochondria, 57 (2018)
989 11943–11946. <https://doi.org/10.1002/anie.201805955>.
- 990 [80] J. Fang, H. Nakamura, A.K. Iyer, Tumor-targeted induction of oxystress for cancer
991 therapy, *Journal of Drug Targeting*. 15 (2007) 475–86.
992 <https://doi.org/10.1080/10611860701498286>.
- 993 [81] M. Viola-Rhenals, K.R. Patel, L. Jaimes-Santamaria, G. Wu, J. Liu, Q.P. Dou, Recent
994 Advances in Antabuse (Disulfiram): The Importance of its Metal-binding Ability to its
995 Anticancer Activity, *Current Medicinal Chemistry*. 25 (2018) 506–524.
996 <https://doi.org/10.2174/0929867324666171023161121>.
- 997 [82] Q. Pan, B. Zhang, X. Peng, S. Wan, K. Luo, W. Gao, Y. Pu, B. He, A dithiocarbamate-
998 based H(2)O(2)-responsive prodrug for combinational chemotherapy and oxidative
999 stress amplification therapy, *Chemical Communications (Cambridge, England)*. 55
1000 (2019) 13896–13899. <https://doi.org/10.1039/c9cc05438c>.
- 1001 [83] J. Noh, B. Kwon, E. Han, M. Park, W. Yang, W. Cho, W. Yoo, G. Khang, D. Lee,
1002 Amplification of oxidative stress by a dual stimuli-responsive hybrid drug enhances
1003 cancer cell death, *Nature Communications*. 6 (2015) 6907.
1004 <https://doi.org/10.1038/ncomms7907>.
- 1005 [84] J. Li, A. Dirisala, Z. Ge, Y. Wang, W. Yin, W. Ke, K. Toh, J. Xie, Y. Matsumoto, Y.
1006 Anraku, K. Osada, K. Kataoka, Therapeutic Vesicular Nanoreactors with Tumor-Specific
1007 Activation and Self-Destruction for Synergistic Tumor Ablation, *Angewandte Chemie*
1008 *(International Ed. in English)*. 56 (2017) 14025–14030.
1009 <https://doi.org/10.1002/anie.201706964>.
- 1010 [85] P.C. Trippier, C. McGuigan, Boronic acids in medicinal chemistry: anticancer,
1011 antibacterial and antiviral applications, *MedChemComm*. 1 (2010) 183–198.
1012 <https://doi.org/10.1039/C0MD00119H>.
- 1013 [86] J. Plescia, N. Moitessier, Design and discovery of boronic acid drugs, *European Journal*
1014 *of Medicinal Chemistry*. 195 (2020) 112270.
1015 <https://doi.org/10.1016/j.ejmech.2020.112270>.
- 1016 [87] K.A. Andersen, T.P. Smith, J.E. Lomax, R.T. Raines, Boronic Acid for the Traceless
1017 Delivery of Proteins into Cells, *ACS Chemical Biology*. 11 (2016) 319–23.
1018 <https://doi.org/10.1021/acschembio.5b00966>.
- 1019 [88] G.A. Ellis, M.J. Palte, R.T. Raines, Boronate-mediated biologic delivery, *Journal of the*
1020 *American Chemical Society*. 134 (2012) 3631–4. <https://doi.org/10.1021/ja210719s>.
- 1021 [89] P. Liu, B. Xu, J. Quilley, P.Y. Wong, Peroxynitrite attenuates hepatic ischemia-
1022 reperfusion injury, *American Journal of Physiology. Cell Physiology*. 279 (2000) C1970-
1023 7. <https://doi.org/10.1152/ajpcell.2000.279.6.C1970>.
- 1024 [90] C. Szabó, H. Ischiropoulos, R. Radi, Peroxynitrite: biochemistry, pathophysiology and
1025 development of therapeutics, *Nature Reviews. Drug Discovery*. 6 (2007) 662–80.
1026 <https://doi.org/10.1038/nrd2222>.
- 1027 [91] T.P. Szatrowski, C.F. Nathan, Production of large amounts of hydrogen peroxide by
1028 human tumor cells, *Cancer Research*. 51 (1991) 794–8.

- 1029 [92] W.C. Xu, J.Z. Liang, C. Li, Z.X. He, H.Y. Yuan, B.Y. Huang, X.L. Liu, B. Tang, D.W.
1030 Pang, H.N. Du, Y. Yang, Pathological hydrogen peroxide triggers the fibrillization of
1031 wild-type SOD1 via sulfenic acid modification of Cys-111, 9 (2018) 67.
1032 <https://doi.org/10.1038/s41419-017-0106-4>.
- 1033 [93] G.P. Bienert, J.K. Schjoerring, T.P. Jahn, Membrane transport of hydrogen peroxide,
1034 *Biochimica et Biophysica Acta*. 1758 (2006) 994–1003.
1035 <https://doi.org/10.1016/j.bbamem.2006.02.015>.
- 1036 [94] B. D'Autréaux, M.B. Toledano, ROS as signalling molecules: mechanisms that generate
1037 specificity in ROS homeostasis, *Nature Reviews Molecular Cell Biology*. 8 (2007) 813–
1038 824. <https://doi.org/10.1038/nrm2256>.
- 1039 [95] A.D. Brooks, K. Yeung, G.G. Lewis, S.T. Phillips, A Strategy for Minimizing Background
1040 Signal in Autoinductive Signal Amplification Reactions for Point-of-Need Assays,
1041 *Analytical Methods : Advancing Methods and Applications*. 7 (2015) 7186–7192.
1042 <https://doi.org/10.1039/c5ay00508f>.
- 1043 [96] J. Liu, S. Zheng, V.L. Akerstrom, C. Yuan, Y. Ma, Q. Zhong, C. Zhang, Q. Zhang, S.
1044 Guo, P. Ma, E.V. Skripnikova, M.R. Bratton, A. Pannuti, L. Miele, T.E. Wiese, G. Wang,
1045 Fulvestrant-3 Boronic Acid (ZB716): An Orally Bioavailable Selective Estrogen Receptor
1046 Downregulator (SERD), *Journal of Medicinal Chemistry*. 59 (2016) 8134–40.
1047 <https://doi.org/10.1021/acs.jmedchem.6b00753>.
- 1048 [97] C. Zhang, S. Guo, L. Yang, J. Liu, S. Zheng, Q. Zhong, Q. Zhang, G. Wang,
1049 Metabolism, pharmacokinetics, and bioavailability of ZB716, a Steroidal Selective
1050 Estrogen Receptor Downregulator (SERD), *Oncotarget*. 8 (2017) 103874–103889.
1051 <https://doi.org/10.18632/oncotarget.21808>.
- 1052 [98] L. Luo, Q. Zhong, S. Guo, C. Zhang, Q. Zhang, S. Zheng, L. He, G. Wang,
1053 Development of a bioavailable boron-containing PI-103 Bioisostere, PI-103BE,
1054 *Bioorganic & Medicinal Chemistry Letters*. 30 (2020) 127258.
1055 <https://doi.org/10.1016/j.bmcl.2020.127258>.
- 1056 [99] Wang et al., Boron-based prodrug strategy for increased bioavailability and lower-
1057 dosage requirements for drug molecules containing at least one phenol (or aromatic
1058 hydroxyl) group, Patent WO2016/004166. (2016).

